JOURNAL OF COMPUTATIONAL PHYSICS **86**, 18–55 (1990)

Kinetic Boundary Layers, Numerical Simulations

PHILIPPE ROSTAND

INRIA, BP 105, 78153 Le Chesnay Cedex, France

Received March 18, 1988; revised November 30, 1988

We take interest here in nonequilibrium boundary layers for polytropic viscous flows. A quick physical introduction is given, then we propose an extension of an existing numerical scheme for the compressible Navier–Stokes equations to take into account slip-boundary conditions; 2-dimensional numerical simulations are presented. © 1990 Academic Press, Inc.

INTRODUCTION

The prediction of temperature on space shuttles, and more generally on supersonic and hypersonic airplanes, has raised the need for a precise description of physical phenomena within the proximity of obstacles.

Comparison of numerical simulations with experimental data (see, for example, [1]) has shown that compressible Navier–Stokes equations with the usual no-slip boundary conditions do not give an accurate shock in the case of rarefied gas flows, which is our concern for the study of a space vehicle entering the atmosphere.

This is due to the fact that the equations of fluid dynamics (compressible Euler or Navier–Stokes) are an approximation to the kinetic description given by the Boltzman equation, valid only when the Knudsen number is small ($\mathrm{Kn} = \lambda/L$, where λ is the local mean free path and L is a local characteristic length of the flow). This is not the case near an obstacle, because L is arbitrarily small (smaller than the distance to the wall). Consequently, there is a small layer, about one mean free path thick, which cannot be described by the fluid equations. In the case of a rarefied flow, this layer has a significant thickness, and we want to consider a nonequilibrium boundary layer, between the body and the fluid flow, and obtain from its study boundary conditions for the latter.

A simplified boundary layer model, which we will use here, has been obtained by Gupta, Scott, and Moss in [2]. Coron, Golse, and Sulem are working on a more elaborate model; preliminary results are shown in [3].

In part I, we will give a short introduction to the Boltzmann equation and to the derivation and validity of the fluid approximation. The boundary layer model, and the derivation of boundary conditions for the Navier–Stokes equations will be outlined in Part II (see [2] for more details). Slip and no-slip conditions are compared from a mathematical point of view in part III, an adaptation of existing numerical methods for the compresible Navier–Stokes equations is proposed in part IV; flow simulations are shown in part V.

0021-9991/90 $3.00

I. Boltzmann Equation and Fluid Approximation

This is only a very quick and simplified introduction to a large subject; further information can be found in the books by C. Bardos [8] for basic outlines, by R. Brun [4], S. Chapman and T. Cowling [5], Truesdell and Muncaster [6] or G. A. Bird [7] (among others) for extensive details.

At the molecular level, a gas is described by calculating the path of every molecule, taking into account its interactions with all the others; of course, numerically this is an impossible task. Statistical models assume that the particles are numerous enough, i.e., that the gas is dense enough, to allow description by a smooth probability function $f(x, v, t)$, defined by

$$m\, dn = f(x, v, t)\, d^3x\, d^3v \tag{1}$$

$$x \in R^3 \text{ position}, \qquad v \in R^3 \text{ speed}, \qquad t \in R^+ \text{ time},$$

where m is the mass of one particle, dn the number of particles having their coordinates in an elementary cell $d^3x \otimes d^3v$ of the state space, here R^6, at a given time t.

Then f satisfies

$$\frac{\partial f}{\partial t} + v \cdot \nabla_x f = C(f), \tag{2}$$

where C is a collision operator.

If we also assume that

— the particles have no electric charge,

— the gas is monoatomic, so that the particles have only three degrees of freedom: the three speed components,

— the gas is not too dense, so that collisions involving more than two particles can be neglected, and the collisions are elastic,

then the collision operator is local in space, and quadratic:

$$C(f) = Q(f, f) = \int_{R^3} \int_{S^2} (f'f'_1 - ff_1)\, q(|v - v_1|, w)\, dw\, dv_1, \tag{3}$$

where

$$f = f(v, v_1, w) = f(x, v, t) \tag{4}$$

$$f_1 = f_1(v, v_1, w) = f(x, v_1, t) \tag{5}$$

$$f' = f'(v, v_1, w) = f(x, v + (v_1 - v, w)\, w, t) \tag{6}$$

$$f'_1 = f'_1(v, v_1, w) = f(x, v_1 - (v_1 - v, w)\, w, t), \tag{7}$$

with $S^2 = \{w \in R^3,\ \|w\| = 1\}$ and q is the diffusion cross section, it depends on the collision modelling chosen.

The Boltzman equations (2)–(7) is difficult to solve because it is an integro-differential equation depending on six variables (seven if the problem is time dependent). Probabilistic and deterministic simulation methods exist (see [7 or 9] for a recent contribution), but they are very expensive. But if our concern is aerodynamics, we do not need the complete kinetic solution f, but only some of its moments: the density $\rho(x, t)$, the momentum $\rho u(x, t)$ and the total energy $E(x, t)$,

$$\rho(x, t) = \int_{R^3} f(x, v, t)\, d^3v \tag{8}$$

$$(\rho u)_i(x, t) = \int_{R^3} v_i f(x, v, t)\, d^3v, \qquad i = 1, 2, 3 \tag{9}$$

$$E(x, t) = \int_{R^3} \frac{|v|^2}{2} f(x, v, t)\, d^3v. \tag{10}$$

The problem of fluid approximation is to find approximate equations giving ρ, ρu, and E without solving the Boltzman equation.

The collision being elastic, mass momentum and energy are conserved in a collision. This implies that

$$\int Q(f, f)\, d^3v = 0 \tag{11}$$

$$\int Q(f, f)\, v_i\, d^3v = 0 \tag{12}$$

$$\int Q(f, f) \frac{|v|^2}{2} d^3v = 0 \tag{13}$$

as can be checked directly; 1, v_i, $|v|^2/2$ are the summational invariants. Integrating (2) over the velocity space, one obtains

$$\frac{\partial \rho}{\partial t} + \operatorname{div}(\rho u) = 0. \tag{14}$$

Multiplying (2) by v_i and integrating, one obtains

$$\frac{\partial}{\partial t}(\rho u)_i + \sum_j \frac{\partial}{\partial x_j}\left(\int_{R^3} v_i v_j f\, d^3v\right) = 0. \tag{15}$$

Multiplying by $|v|^2/2$, and integrating, one obtains

$$\frac{\partial}{\partial t} E + \sum_i \frac{\partial}{\partial x_i}\left(\int_{R^3} \frac{|v|^2}{2} v_i f\, d^3v\right) = 0. \tag{16}$$

By using

$$u_i(x, t) = \frac{\int f(x, v, t)\, v_i\, d^3v}{\int f(x, v, t)\, d^3v} \tag{17}$$

and for a given x and t, $c_i = v_i - u_i$, one can rewrite (15) as

$$\frac{\partial(\rho u)}{\partial t} + \operatorname{div}(\rho u \otimes u) + \operatorname{div}(\tau) = 0, \tag{18}$$

where τ is the stress tensor, defined by

$$\tau_{i,j} = \int c_i c_j f(x, v, t)\, d^3v. \tag{19}$$

One can rewrite (16) as

$$\frac{\partial E}{\partial t} + \operatorname{div}(Eu) + \operatorname{div}(u \cdot \tau) + \operatorname{div} q = 0, \tag{20}$$

where q is heat flux vector

$$q_i = \int \frac{|v|^2}{2} c_i f(x, v, t)\, d^3v. \tag{21}$$

These equations are the conservation laws; they involve ρ, ρu, and E, but also other moments of f. It is necessary to obtain expressions of these moments depending only on ρ, ρu, and E and of their derivatives: we want a closing relation for (14), (15), (16).

In order to do that, we go back to the Boltzman equation. One can show by taking the continuous limit of a discrete model that the probability of a state $\{f(x, v, t),\ x \in R^3,\ v \in R^3\}$ is given by the opposite of Boltzman's H function:

$$H(t) = -\iint_{R^6} f \operatorname{Log} f\, d^3x\, d^3v. \tag{22}$$

H can be shown to be decreasing in time for an isolated system: it is an entropy. The state with the minimum entropy is the most probable state; it is necessarily a Maxwellian,

$$M(x, v, t) = \frac{\rho}{(2\pi(kT/m))^{3/2}} \exp\left(-\frac{|v-u|^2}{2(kT/m)}\right), \tag{23}$$

where ρ, u, and T are the density, the average speed, and the temperature, and where k is Boltzmann's constant, m is the mass of the molecules.

Such a state is said to be at equilibrium; one may suppose that f is locally "not far" from a Maxwellian when there are no perturbations (shocks, walls, initial

layers, etc.) near the point under consideration. This is the base of the Chapman–Enskog expansion: one tries to find f as a Maxwellian plus a small perturbation.

The zero-order expansion is obtained by supposing that f is a Maxwellian

$$f(x, v, t) = M(x, v, t). \tag{24}$$

Replacing f by M in (19), one obtains

$$\tau_{ij} = \rho(x, t) T(x, t)\, \delta_{i,j} = p(x, t)\, \delta_{i,j};$$

p: pressure.

Replacing f by M in (21), one obtains $q = 0$.

So (14), (18), and (20) are now the compressible conservative Euler equations:

$$\frac{\partial \rho}{\partial t} + \operatorname{div}(\rho u) = 0 \tag{25}$$

$$\frac{\partial(\rho u)}{\partial t} + \operatorname{div}(\rho u \otimes u) + \nabla p = 0 \tag{26}$$

$$\frac{\partial E}{\partial t} + \operatorname{div}((E + p)u) = 0. \tag{27}$$

To have a more accurate result, we suppose that

$$f = M(1 + \varepsilon\phi), \qquad \phi = \phi(x, v, t), \tag{28}$$

where $\varepsilon = 1/Kn$.

The nondimensionalized Boltzman equation can be written as

$$\frac{\partial f^*}{\partial t} + v^* \cdot \nabla_x f^* = \frac{1}{\varepsilon} Q(f^*, f^*); \tag{29}$$

replacing f^* by $M^*(1 + \varepsilon\phi)$, we obtain

$$-\frac{1}{\varepsilon}[Q(M^*, M^*)] + \left(\frac{\partial M^*}{\partial t} + v^* \cdot \nabla_x M^* - 2Q(M^*, M^*\phi)\right) + \varepsilon F(M) = 0.$$

Supposing the factor of order $1/\varepsilon$ to be zero, we obtain $Q(M^*, M^*) = 0$, which is equivalent to M^* being a Maxwellian: we again find that the lowest order approximation is a Maxwellian.

By equating the factor of order zero to be zero, we obtain

$$\frac{\partial M^*}{\partial t} + v \cdot \nabla_x M^* - 2Q(M^*, M^*\phi) = 0. \tag{30}$$

This is a Fredholm integral equation for ϕ, the orthogonality of the left-hand side expression to the null space of the operator gives the Euler equations.

The equation (30) is difficult to solve and does not yield useful results because the expression for ϕ is too complicated. But one can obtain a good approximation of the solution by taking ϕ as a linear combination of two special eigenvectors of the operator: the two first Sonine polynomials.

After some calculations, one obtains

$$\phi = -\frac{1}{K}\frac{\sqrt{\pi}}{\rho}\frac{5}{8}\sqrt{\frac{m}{kT}}\left(\frac{3}{2}\frac{1}{T}\nabla T\cdot c\left(\frac{mc^2}{2kT}-\frac{5}{2}\right)\right.$$
$$\left.+\frac{m}{kT}\left(c\otimes c-\frac{1}{3}c^2 I\right):(\nabla u)\right), \tag{31}$$

where K is a normalization constant.

Equation (19) then gives

$$\tau = \left(\int c_i c_j M(1+\varepsilon\phi)\right)_{i,j}$$
$$= 2\mu[\tfrac{1}{2}(\nabla u+\nabla u^t)-\tfrac{1}{3}(\operatorname{div}(u))I]+p, \tag{32}$$

where μ is the first viscosity,

$$\mu = -\frac{5}{8}\frac{\sqrt{\pi}}{K}m\left(\frac{kT}{m}\right)^{1/2}, \tag{33}$$

for a Maxwellian interaction potential.

Equation (21) gives

$$q = \chi\nabla T \tag{34}$$

$$\chi = -\frac{75}{32}\frac{\sqrt{\Pi}}{K}k\left(\frac{kT}{m}\right)^{1/2}, \tag{35}$$

where χ is the heat diffusion coefficient; (14), (18), and (20) are now the conservative compressible Navier–Stokes equations

$$\frac{\partial\rho}{\partial t}+\operatorname{div}(\rho u)=0 \tag{36}$$

$$\frac{\partial(\rho u)}{\partial t}+\operatorname{div}(\rho u\otimes u)+\nabla p$$
$$=\operatorname{div}\left(-\mu\left((\nabla u+\nabla u^t)-\frac{2}{3}\operatorname{div}(u)I\right)\right) \tag{37}$$

$$\frac{\partial E}{\partial t}+\operatorname{div}[(E+p)u]$$
$$=\operatorname{div}\left[u\cdot\left(-\mu\left((\nabla u+\nabla u^t)-\frac{2}{3}\operatorname{div}(u)\right)\right)\right]+\operatorname{div}(-\chi\nabla T). \tag{38}$$

Remark. These values for μ and λ are valid only for a monoatomic gas with a Maxwellian interaction potential. For a diatomic or a triatomic gas, a similar theory can be developed, but it is much more complicated because the diffusion cross section is not spheric.

The Chapman–Enskog approximation is obviously not valid in the neighborhood of a wall, a sufficient reason for that being the anisotropy introduced by the obstacle.

II. Nonequilibrium Boundary Layer Models

The general problem of boundary layers is to derive boundary conditions (see Fig. 1) for the fluid flow from an assumed behavior of the particles when they hit the wall. The usual formulation of this problem is shown in Fig. 2.

Given a set of fluid variables at the edge of the Knudsen layer ρ_s, $(\rho u)_s$, E_s, the corresponding Navier–Stokes probability function $f_s = M_s(1 + \varepsilon_s \phi_s)$ is known and consequently the incident fluxes: for $\phi_i = 1, v_x, v_y, v_z, |v|^2/2$,

$$F_i = \int_{-\infty}^{+\infty} \int_{-\infty}^{0} \int_{-\infty}^{+\infty} v_y \phi_i f_s(v)\, d^3v.$$

Rescaling the problem by $1/\lambda$, the calculation of the reflected fluxes R_i is a classical half space problem (see [3 or 10]). The boundary conditions are given by equating the sum of the incident and reflected fluxes to the known boundary flux

$$F_i + R_i = G_i \tag{39}$$

with

$$G_i = \int_{-\infty}^{+\infty} \int_{-\infty}^{+\infty} \int_{-\infty}^{+\infty} v_y \phi_i f_s(v)\, d^3v. \tag{40}$$

To avoid resolving the half space problem, one makes assumptions on the behavior of f in the Knudsen layer.

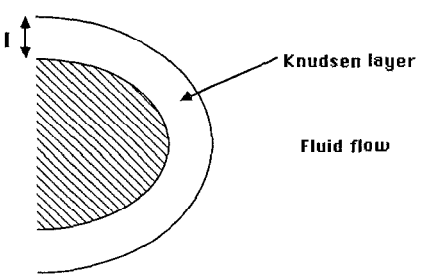

Figure 1

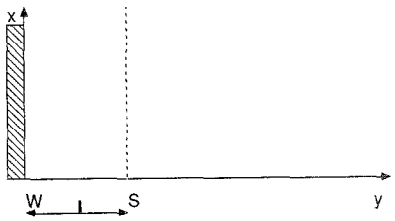

FIGURE 2

We reproduce here the main points of the rationale developed by Gupta, Scott, and Moss in [2]. They assume that:

— a proportion θ of the particles hitting the wall is accomodated and re-emitted according to a Maxwellian law, the rest is specularly reflected (θ is the accomodation coefficient),

— the fluxes are constant during a "one-way travel" through the Knudsen layer.

The second hypothesis is a very strong one; it rules out shock-boundary layer interaction. In this context,

$$R_i = (1-\theta)\int_{-\infty}^{+\infty}\int_{0}^{+\infty}\int_{-\infty}^{+\infty} v_y \phi_i f_s(v_x, -v_y, v_z)\, d^3v$$

$$+\theta\int_{-\infty}^{+\infty}\int_{-\infty}^{+\infty}\int_{-\infty}^{+\infty} v_y \phi_i f_w(v)\, d^3v, \tag{41}$$

where

$$f_w(x, v, t) = \frac{\rho_w(x, t)}{(2\pi(kT_w(x, t)/m))^{3/2}} \exp\left(\frac{-|v|^2}{2(kT_w(x, t)/m)}\right) \tag{42}$$

Equation (39) then gives the following boundary conditions, when f_s is replaced by its value, and after simplification,

$$u_x^s = \frac{2-\theta}{\theta}\frac{5\pi}{16}\lambda_s n \cdot D(u_s)\cdot \tau_x \tag{43}$$

$$u_z^s = \frac{2-\theta}{\theta}\frac{5\pi}{16}\lambda_s n \cdot D(u_s)\cdot \tau_z, \tag{44}$$

where s indices refer to the values at the surface between the Knudsen layer and the fluid flow, n is the inward unit vector, τ_x and τ_z are the two tangential normalized vectors,

$$D(u) = \nabla u + \nabla u^t - \tfrac{2}{3}\operatorname{div}(u) I$$

$$\frac{p^s}{p^w} = \left(1 - \left[\frac{2-\theta}{\theta}\frac{15}{16}\frac{\lambda}{T}\frac{\partial T}{\partial n} + \frac{5}{12}\frac{\sqrt{\pi}}{2}\frac{\lambda}{\sqrt{RT_s}} \times \left(\frac{\partial(u\cdot\tau_x)}{\partial x} + \frac{\partial(u\cdot\tau_z)}{\partial z} - 2\frac{\partial(u\cdot n)}{\partial n}\right)\right]\right)_s^{-1} \tag{45}$$

$$= \frac{T_s}{T_w} = \frac{1}{2}\left(\frac{P_y}{p^s} + 1\right) \times \left[-\frac{1}{2} + \frac{3}{4}\left(\frac{P_y}{p^s} + 1\right) - \frac{75\pi}{128}\frac{2-\theta}{\theta}\left(\frac{\lambda}{T}\frac{\partial T}{\partial y}\right)\right]_s^{-1}, \tag{46}$$

where P_y is the normal momentum flux.

Only (40) and (41) are useful for the fluid calculation if T_w is unknown; (42) and (43) allow calculation of the pressure and temperature on the wall once the fluid flow is known.

More accurate models are under investigation at the École Normale Supérieure (Bardos *et al.*); they introduce a boundary layer term χ in the Chapman–Enskog expansion: if the wall is located at $x = 0$,

$$f = M(1 + \varepsilon\phi) + \chi\left(\frac{x}{\varepsilon}, v, t\right).$$

By rescaling the equation, one obtains a half-space problem for χ, the well-posedness of which implies the necessary conditions for $M(1+\varepsilon\phi)$ and, consequently, boundary conditions for the fluid flow. Preliminary results [3] show that the boundary conditions obtained are of the same kind, but with coefficients which are more reliable than those above.

III. The Compressible Navier–Stokes Equation with Slip Boundary Conditions

We restrict ourselves to the 2-dimensional case for simplicity, and we assume the viscosity and heat diffusion coefficients to be constant (see Fig. 3), where $O \in R^2$

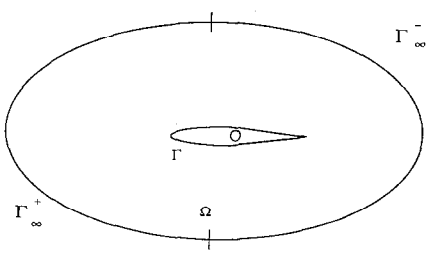

FIGURE 3

represents the obstacle, Ω the flow domain, $\Gamma = \partial O$, $\Gamma_\infty = \partial\Omega/\Gamma$. The nondimensionalized Navier–Stokes system is then

$$\frac{\partial \rho}{\partial t} + \operatorname{div}(\rho u) = 0 \tag{44}$$

$$\frac{\partial(\rho u)}{\partial t} + \operatorname{div}(\rho u \otimes u) + \nabla p = \frac{1}{\mathrm{Re}} \operatorname{div}(D(u)) \tag{45}$$

$$\frac{\partial E}{\partial t} + \operatorname{div}((E+p)u) = \frac{1}{\mathrm{Re}}\left(\operatorname{div}(u(D(u)) + \frac{\gamma}{\mathrm{Pr}} \Delta T\right) \tag{46}$$

in Ω, where

$u \in R^2$ is the speed

$p = (\gamma - 1)\rho T$ is the pressure,

Re is the Reynolds number at infinity,

Pr is the Prandtl number,

with boundary conditions on Γ,

$$u \cdot n = 0 \tag{47}$$

$$n \cdot D(u) \cdot \tau = -A\rho u \cdot \tau \tag{48}$$

$$\frac{1}{\mathrm{Re}} u \cdot D(u) \cdot n + \frac{\gamma}{\mathrm{Pr}\,\mathrm{Re}} \frac{\partial T}{\partial n} = 0, \tag{49}$$

where n is the outward normal unit vector to Γ, τ a unit vector tangential to Γ, and $D(u) = \nabla u + \nabla u^t - \frac{2}{3}\nabla \cdot uI$.

Equation (47) is a natural boundary condition, assuming there is no mass flux through the Knudsen layer. Equation (48) is given by (40) and (41); A is a positive constant, depending on the nature of the gas in consideration and on its density

$$A = \rho_\infty c, \tag{50}$$

where c is a physical constant, $c \cong 10^7$ U.S.I. for air, and ρ_∞ is the physical density of the gas for away from the body, $\rho_\infty = 1, 2\,\mathrm{kg\,m^{-3}}$ at ground level, $\rho_\infty = 10^{-7}\,\mathrm{kg\,m^{-3}}$ at an altitude of 120 km. The characterisation of the rarefaction of the flow in Eq. ((47)–(53)) is the free-stream density because the equations are nondimensionalized by taking $\rho = 1$ at the inflow boundary. Of course, the density in the vicinity of the wall might be much higher than the free-stream density, depending on the strength of the shock, so that the slip velocity does not depend on A only, but also on the free-stream Mach number, for example.

Equation (49) is the consequence of the known adiabaticity of the wall. We assume the flow at infinity to be uniform,

$$u = (\cos \alpha, \sin \alpha) \tag{51}$$

$$\rho = 1 \tag{52}$$

$$T = \frac{1}{\gamma(\gamma - 1) M_0^2}, \tag{53}$$

where M_0 is the free-stream Mach number and α is the angle of attack.

In fact, we enforce the boundary conditions (51), (52), (53) totally or partially, according to a local linearized characteristic analysis.

Theoretical results on the compressible Navier–Stokes equations are scarce (see [11] for a local in time result), but one can check a few necessary conditions for the well-posedness of the problem: decay of energy and entropy of a smooth solution, coercivity of the viscous term restricted to the speed space, number of boundary conditions compared to the signature of the convection Jacobian matrix.

We assume the external boundary Γ_∞ to be sufficiently far from the body for the flow to be uniform in its neighborhood; consequently all derivatives of ρ, u, and E are zero on Γ_∞.

The decay of energy is very easily obtained,

$$\frac{d}{dt}\left(\int_\Omega E\right) = -\int_\Omega \nabla \cdot ((E+p)u) + \frac{1}{\mathrm{Re}} \int_\Omega \nabla \cdot (u \cdot D(u)) + \frac{\gamma}{\mathrm{Re\,Pr}} \int_\Omega \Delta T$$

$$= -\int_{\Gamma \cup \Gamma_\infty} (E+p)(u \cdot n) + \int_{\Gamma \cup \Gamma_\infty} \left(\frac{1}{\mathrm{Re}} u \cdot D(u) \cdot n + \frac{\gamma}{\mathrm{Re\,Pr}} \frac{\partial T}{\partial n} \right).$$

On Γ,

$$u \cdot n = 0$$

$$\frac{1}{\mathrm{Re}} u \cdot D(u) \cdot n + \frac{\gamma}{\mathrm{Pr\,Re}} \frac{\partial T}{\partial n} = 0,$$

so the boundary flux is zero.

On Γ_∞, $D(u) = 0$, $\partial T / \partial n = 0$, and $(E+p)(u \cdot n)$ is constant, so

$$\int_{\Gamma_\infty} (E+p)(u \cdot n) = 0,$$

thus

$$\frac{d}{dt}\left(\int_\Omega E\right) = 0.$$

The decay of entropy is slightly more difficult to obtain. The entropy per unit mass is ρs, with

$$s = \mathrm{Log}\left(\frac{\rho^{\gamma-1}}{T}\right). \tag{54}$$

Combining (44), (45), and (46), we obtain

$$\frac{\partial \rho s}{\partial t} + \nabla \cdot (\rho u s) = -\frac{1}{T\,\mathrm{Re}}\left[\frac{\gamma}{\mathrm{Pr}}\Delta T + F(\nabla u)\right] \tag{55}$$

with

$$F(\nabla u) = (\nabla u + \nabla u^t - \tfrac{2}{3}\nabla u) : \nabla u \tag{56}$$

or

$$F(\nabla u) = \frac{4}{3}\left[\left(\frac{\partial v}{\partial x}\right)^2 + \left(\frac{\partial w}{\partial y}\right)^2\right] + \left(\frac{\partial w}{\partial x} + \frac{\partial v}{\partial y}\right)^2 - \frac{4}{3}\frac{\partial v}{\partial x}\frac{\partial w}{\partial y}. \tag{57}$$

If $u = (v, w)$,

$$F(\nabla u) = \frac{2}{3}\left[\left(\frac{\partial v}{\partial x}\right)^2 + \left(\frac{\partial w}{\partial y}\right)^2\right] + \left(\frac{\partial w}{\partial x} + \frac{\partial v}{\partial y}\right)^2 + \frac{2}{3}\left(\frac{\partial v}{\partial x} - \frac{\partial w}{\partial y}\right)^2 \tag{58}$$

$$F(\nabla u) \geqslant 0$$

$$\frac{d}{dt}\left(\int_\Omega \rho s\right) = -\int_\Omega \nabla \cdot (\rho u s) - \frac{1}{\mathrm{Re}}\int_\Omega \frac{F(\nabla u)}{T} - \int_\Omega \frac{1}{\mathrm{Re}}\frac{\gamma}{\mathrm{Pr}}\frac{\Delta T}{T}$$

$$\leqslant -\int_{\Gamma \cup \Gamma_\infty} \rho s (u \cdot n) - \int_\Omega \frac{\gamma}{\mathrm{Re}\,\mathrm{Pr}}\frac{|\nabla T|^2}{T^2} - \int_{\Gamma \cup \Gamma_\infty} \frac{\gamma}{\mathrm{Re}\,\mathrm{Pr}}\frac{1}{T}\frac{\partial T}{\partial n}.$$

On Γ,

$$u \cdot n = 0$$

$$\frac{\gamma}{\mathrm{Re}\,\mathrm{Pr}}\frac{\partial T}{\partial n} = -\frac{1}{\mathrm{Re}}\, u \cdot D(u) \cdot n.$$

But on Γ, $u = (u \cdot \tau)\tau$, so that

$$\frac{\gamma}{\mathrm{Re}\,\mathrm{Pr}}\frac{\partial T}{\partial n} = -\frac{1}{\mathrm{Re}}\,(u \cdot \tau)\tau \cdot D(u) \cdot n.$$

Using (48),

$$\frac{\gamma}{\mathrm{Re}\,\mathrm{Pr}}\frac{\partial T}{\partial n} = \frac{A}{\mathrm{Re}}\,\rho (u \cdot \tau)^2 \geqslant 0. \tag{59}$$

On Γ_∞, $\partial T/\partial n = 0$, $\rho s(u \cdot n)$ is constant, so we obtain

$$\frac{d}{dt}\left(\int_\Omega \rho s\right) \leqslant 0. \tag{60}$$

Coercivity of the Viscous Term

The following results are extensions of R. Verfurth's work on the incompressible case (see [12]). The question is on the existence and uniqueness of a solution $u \in (H^1(\Omega))$ of

$$-\operatorname{div}(D(u)) = g \qquad \text{in } \Omega \tag{61a}$$

$$u \cdot n = 0 \qquad \text{in } \Gamma \tag{61b}$$

$$n \cdot D(u) \cdot \tau = -A(u \cdot \tau) \qquad \text{in } \Gamma \tag{61c}$$

for Ω bounded domain of R^2, $g \in L^2(\Omega)$, where A is a positive constant, n is the outward normal unit vector to $\partial\Omega$, and τ is a tangential vector to $\partial\Omega$.

Let $V = \{u \in H^1(\Omega)^2,\ u \cdot n = 0 \text{ on } \partial\Omega\}$. If we assume $\partial\Omega$ to be regular (say C^1), the function

$$n: \partial\Omega \to R^2$$
$$x \to n(x)$$

is C^1 and, consequently, the trace operator

$$H^1(\Omega) \to H^{1/2}(\Gamma)$$
$$u \to u \cdot n$$

is continuous (see [12] for details). So V with the $H^1(\Omega)$ norm, as a closed subspace of $H^1(\Omega)$, is a Hilbert space.

Let $\phi \in V$; (61) implies, integrating by parts,

$$\frac{1}{2}\int_\Omega D(u) \cdot D(\phi) + \int_\Omega \frac{2}{9}\nabla \cdot u \nabla \cdot \phi - \int_\Gamma \phi \cdot D(u) \cdot \tau = \int_\Omega g\phi. \tag{62}$$

$\int_\Gamma \phi \cdot D(u) \cdot \tau$ is a well-defined integral if we take u such that $-\operatorname{div}(D(u)) \in L^2(\Omega)$, because then $n \cdot D(u)|_\Gamma \in H^{-1/2}(\Gamma)$.

Equation (61c) then implies

$$\forall \psi \in H^{1/2}(\Gamma), \qquad \int_\Gamma (n \cdot D(u) \cdot \tau + Au \cdot \tau)\psi = 0$$

$$\Leftrightarrow \forall \phi \in V, \qquad \int_\Gamma (n \cdot D(u) \cdot \tau + Au \cdot \tau) \cdot (\phi \cdot \tau) = 0.$$

Equation (62) then implies

$$\forall \phi \in V \qquad \frac{1}{2}\int_\Omega D(u)D(\phi) + \frac{2}{9}\int_\Omega \nabla\cdot u \nabla\cdot\phi + A\int_\Gamma (\phi\cdot\tau)(u\cdot\tau) = \int_\Omega g\cdot\phi. \quad (63)$$

Conversely, it is well known that (63) and $u \in V$ imply (61); (63) first implies that $-\operatorname{div}(D(u)) = g$ in the distribution sense, so that $\operatorname{div}(D(u)) \in L^2(\Omega)$, and consequently we have the boundary condition (61c) in $H^{-1/2}(\Gamma)$.

To use Lax–Milgram's theorem, we must prove the coercivity of the bilinear form ϕ;

$$\phi\colon V \to R$$

$$u \to \frac{1}{4}\int_\Omega |D(u)|^2 + \frac{1}{9}\int_\Omega (\nabla\cdot u)^2 + \frac{A}{2}\int_\Gamma (u\cdot\tau)^2.$$

Where we recall that A is a strictly positive constant,

$$|D(u)|^2 = |\nabla u + \nabla u^t - \tfrac{2}{3}\nabla\cdot u I|^2 = |\nabla u + \nabla u^t|^2 - \tfrac{16}{9}(\nabla\cdot u)^2$$

$$\tfrac{1}{4}|D(u)|^2 + \tfrac{1}{9}(\nabla\cdot u)^2 = \tfrac{1}{4}|\nabla u + \nabla u^t|^2 - \tfrac{1}{3}(\nabla\cdot u)^2.$$

If $u = (v, w)$,

$$(\nabla\cdot u)^2 \leqslant 2\left[\left(\frac{\partial v}{\partial x}\right)^2 + \left(\frac{\partial w}{\partial y}\right)^2\right]$$

$$|\nabla u + \nabla u^t|^2 \geqslant 4\left(\frac{\partial v}{\partial x}\right)^2 + 4\left(\frac{\partial w}{\partial y}\right)^2.$$

So $\forall u \in H^1(\Omega)$,

$$\tfrac{1}{4}|D(u)|^2 + \tfrac{1}{9}(\operatorname{div} u)^2 \geqslant \tfrac{1}{12}|\nabla u + \nabla u^t|^2. \quad (64)$$

We will now recall two classical lemmas.

LEMMA 1 (Korn's inequality). *There are two positive constants, depending on Ω, such that*

$$\forall u \in H^1(\Omega), \qquad \frac{1}{2}\int_\Omega |\nabla u + \nabla u^t|^2 \leqslant C_1\|u\|^2_{H^1(\Omega)} - C_2\|u\|_{L^2(\Omega)}. \quad (65)$$

A proof is given in [13].

LEMMA 2 (Poincaré–Morrey). *There is a constant $C_3(\Omega)$, strictly positive, such that*

$$\forall u \in H^1(\Omega), \qquad C_3(\Omega)\,\|u\|_{L^2(\Omega)} \leqslant \int_\Omega |\nabla u + \nabla u^t|^2 + \int_\Gamma |u\cdot n|^2 + \int_\Gamma |u\cdot\tau|^2. \quad (66)$$

Proof. See [12, Lemma 2.2].

PROPOSITION 1. *ϕ is coercive.*

Proof. (64), (65), and (66) imply $\phi(u) \geqslant C\|u\|_{H^1(\Omega)}$ $\forall u \in V$, if $C \leqslant (C_1/12)(1/2 + C_2/C_3)$ and $C \leqslant A(C_3/C_2)$. So, by Lax–Milgram's theorem, (61) has a unique solution.

It is easy to check that no such result exists in three dimensions.

Weak Formulation of (44)–(49), (51)–(53)

It is well known that the boundary condition $u \cdot n = 0$ cannot be enforced strongly on a polygonal domain: if, for example, u is piecewise linear, if s is a corner of the boundary, $u_s \cdot n_1 = 0$, $u_s \cdot n_2 = 0$, so $u_s = 0$. This means $u = 0$ on the boundary. Consequently, we will take a weak formulation in $(H^1(\Omega))^4$.

Let ϕ, $\varepsilon \in H^1(\Omega)$, $\psi \in H^1(\Omega)^2$, (44)–(49), (51)–(53) be equivalent to

$$\frac{\partial}{\partial t}\int_\Omega \rho\phi - \int_\Omega \rho u \cdot \nabla\phi + \int_{\Gamma_\infty} \rho_0(u_0 \cdot n)\phi = 0 \tag{67}$$

$$\begin{aligned}
&\frac{\partial}{\partial t}\int_\Omega \rho u \cdot \psi - \int_\Omega \rho(u \cdot \nabla\psi \cdot u) + \int_{\Gamma_\infty} \rho_0(u_0 \cdot n)(u \cdot \psi) \\
&\quad - \int_\Omega P\nabla \cdot \psi + \int_{\Gamma_\infty} P_0\psi \cdot n + \int_\Gamma P\psi \cdot n \\
&= -\frac{1}{\mathrm{Re}}\int_\Omega D(u) : \nabla\psi + \frac{1}{\mathrm{Re}}\int_{\Gamma_\infty} n \cdot D(u) \cdot \psi \\
&\quad - \frac{A}{\mathrm{Re}}\int_\Gamma \rho(u \cdot \tau)(\psi \cdot \tau) + \frac{1}{\mathrm{Re}}\int_\Gamma (n \cdot D(u) \cdot n)(\psi \cdot n)
\end{aligned} \tag{68}$$

$$\begin{aligned}
&\frac{\partial}{\partial t}\int_\Omega E\varepsilon - \int_\Omega (E + p)\, u \cdot \nabla\varepsilon + \int_{\Gamma_\infty} (E_0 + p_0)(u \cdot n)\varepsilon \\
&\quad = -\frac{1}{\mathrm{Re}}\int_\Omega u \cdot D(u) \cdot \nabla\varepsilon - \frac{\gamma}{\mathrm{Pr}\,\mathrm{Re}}\int_\Omega \nabla T \cdot \nabla\varepsilon \\
&\quad + \frac{1}{\mathrm{Re}}\int_{\Gamma_\infty} \left(u \cdot D(u) \cdot n + \frac{\gamma}{\mathrm{Pr}}\frac{\partial T}{\partial n}\right)\varepsilon,
\end{aligned} \tag{69}$$

where u_0, ρ_0, T_0, E_0, P_0 are u_∞, ρ_∞, T_∞, E_∞, p_∞ or u, ρ, T, E, P depending on the signature of the jacobian matrix of the convective terms (see [14 or 15] for details).

IV. Numerical Method

Efficient finite element methods have been developed in the recent years for the compressible Navier-Stokes equations (see [14, 15]). They rely on centered Galerkin approximation with artificial viscosity or upwind finite volume solvers, for the Euler equations (see [16, 17]). We will only outline these methods here.

The functional space $(H^1(\Omega))^4$ is approximated by $(P^1(\Omega_h))^4$, where Ω_h is a polygonal approximation of Ω, and $P_1(\Omega_h)$ is the space of piecewise linear functions on a standard triangulation of Ω_h. The discretized variational formulation then reads

$$\frac{\partial}{\partial t}\int_{\Omega} w_h\phi_h = E(w_h, \phi_h) + N(w_h, \phi_h) \qquad \forall \phi_h \in (P^1(\Omega_h))^4, \tag{70}$$

where

$$w_h = \{\rho_h, (\rho u)_h, (\rho v)_h, E_h\}.$$

$E(w_h, \phi_h)$ stands for the convection terms, depending on the approximation chosen (we usually take an upwind Osher approximation, see [18]), $N(w_h, \phi_h)$ stands for the diffusion terms

$$N(w_h, \phi_h) = N_1(w_h, \phi_h^1) + N_2(w_h, \phi_h^2) + N_3(w_h, \phi_h^3) + N_4(w_h, \phi_h^4) \tag{71}$$

with

$$N_1(w_h, \phi_h^1) = 0 \tag{72}$$

$$\begin{aligned} N_2(w_h, \phi_h^2) + N_3(w_h, \phi_h^3) = & -\frac{1}{\mathrm{Re}}\int_{\Omega_h} D(u_h)\cdot\nabla(\phi_h^2, \phi_h^3) \\ & -\frac{A}{\mathrm{Re}}\int_{\Gamma_h} \rho_h(u_h\cdot\tau)((\phi_h^2, \phi_h^3)\cdot\tau) \\ & -\frac{1}{\mathrm{Re}}\int_{\Gamma_h} (n\cdot D(u_h)\cdot n)((\phi_h^2, \phi_h^3)\cdot\tau) \\ & +\frac{1}{\mathrm{Re}}\int_{\Gamma_\infty} n\cdot D(u_h)\cdot(\phi_h^2, \phi_h^3) \end{aligned} \tag{73}$$

$$N_4(w_h, \phi_h^4) = -\frac{1}{\mathrm{Re}}\int_{\Omega_h} u_h\cdot D(u_h)\cdot\nabla\phi_h^4 - \frac{\gamma}{\mathrm{Pr}\,\mathrm{Re}}\int_{\Omega_h}\nabla T_h\cdot\nabla\phi_h^4 \tag{74}$$

where $\phi_h = (\phi_h^i)_{i=1,4}$, u_h and T_h are P^1 approximations of $(\rho u)_h/\rho_h$ and $E_h/\rho_h - 1/2((\rho u)_h)^2/\rho_h^2$, respectively (one can check that u_h and T_h are still first-order approximations of u and T).

One is usually interested in stationary solutions, so classical time discretizations are delta schemes,

$$\int_{\Omega} (M(w_h^{n+1} - w_h^n), \phi_h) = \Delta t[E(w_h^n, \phi_h) + N(w_h^n, \phi_h)], \tag{75}$$

with M the identity operator for an explicit scheme, a linearization of E in most implicit schemes.

Slip boundary conditions introduce a new problem: A is often a large constant, so the system (75) may be ill-conditioned. That is why, while (75) with $M = I - \Delta t\, \partial E$, ∂E being a linearization of E, is quite efficient with no-slip boundary conditions, here it is not: the Courant number is drastically limited for A greater than unity.

We introduce a totally implicit factored scheme,

$$M = (I - \Delta t\, \partial N)(I - \Delta t\, \partial E), \tag{76}$$

where ∂N is a complete linearization of N, including boundary integrals,

$$\begin{aligned}
&\int \partial N(\delta w_h)\, \phi_h \\
&\quad = \frac{1}{\mathrm{Re}} \int_{\Omega_h} D(\delta u_h) \cdot \nabla[\phi_h^2, \phi_h^3] + \frac{A}{\mathrm{Re}} \int_{\Gamma_h} \delta \rho_h (u_h^n \cdot \tau)([\phi_h^2, \phi_h^3] \cdot \tau) \\
&\qquad + \frac{A}{\mathrm{Re}} \int_{\Gamma_h} \rho_h (\delta u_h \cdot \tau)([\phi_h^2, \phi_h^3] \cdot \tau) - \frac{1}{\mathrm{Re}} \int_{\Gamma_h} (n \cdot D(\delta u_h) \cdot n)[\phi_h^2, \phi_h^3] \cdot n \\
&\qquad + \frac{1}{\mathrm{Re}} \int_{\Omega_h} \delta u_h \cdot D(u_h^n) \cdot \nabla \phi_h^4 + \frac{1}{\mathrm{Re}} \int_{\Omega_h} u_h \cdot D(\delta u_h^n) \cdot \nabla \phi_h^4 \\
&\qquad + \frac{\gamma}{\mathrm{Re\ Pr}} \int_{\Omega_h} \nabla(\delta T_h) \cdot \nabla \phi_h^4,
\end{aligned} \tag{77}$$

where $\delta w_h = w_h^{n+1} - w_h^n$.

Equation (76) is solved at each time step in two successive operations:

$$(I - \Delta t\, \partial E)(\delta W_h) = \Delta t[E(w_h^n) + N(w_h^n)] \tag{78}$$

is solved with respect to the conservative variables, and

$$(I - \Delta t\, \partial N)(\delta w_h) = \delta W_h \tag{79}$$

is solved with respect to the nonconservative variables.

Although an improvement over existing methods, (76) is not stable enough to allow very high Mach nuber and low Reynolds flow calculation, which is our goal for the study of a shuttle reentry. A totally implicit scheme with viscous terms calculated from the conservative variables is being developed.

V. Flow Simulations

These computations were performed on the Cray of the C.C.V.R. and on the IBM 3090 of AMD-BA.

Transonic, supersonic, and hypersonic calculations were performed with slip and no-slip boundary conditions, at different densities, around a NACA0012 airfoil and a cylinder; comparison with experimental data taken from [1] is made. In this preliminary study, the emphasis has been made on the effect of the boundary conditions on the continuum flow, outside the Knudsen layer. Particular attention has been given to the shock shape and location.

The first computation made is a flow over a NACA0012 airfoil at a Mach number of 2 and a Reynolds number of 106. Two results are presented: the no-slip flow and the flow at a density of 10^{-5} kg/m^3. The experimental flowfield, at a density of 10^{-7} kg/m^3, taken from [1], are superimposed. The isodensity lines are shown on Fig. 4. The experimental data is displayed on the upper half of the profile only, in a thicker and darker line. It appears that slip boundary conditions improve the precision of numerical results, although the closest to experiment result is

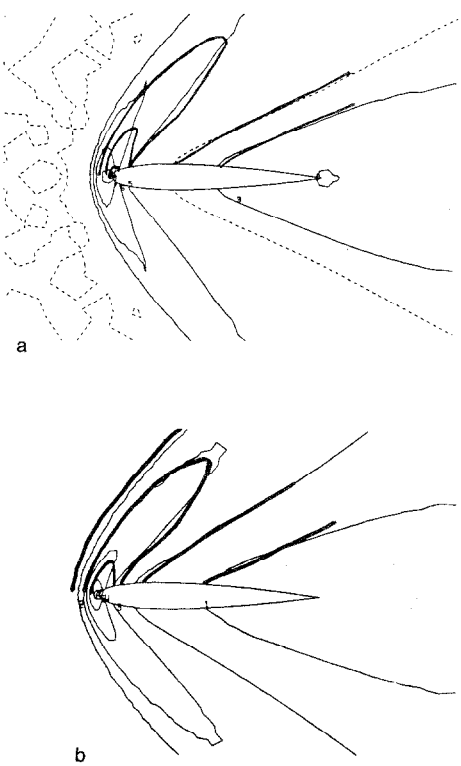

FIG. 4. (a) No-slip iso-density lines. (b) Slip iso-density lines.

obtained for $\rho_\infty = 10^{-5}\,\mathrm{kg/m^3}$, which is not the experimental density. The accommodation coefficient was taken to be $\theta = 0.4$.

A transsonic flow over a NACA0012 airfoil is presented. The Mach number is 0.85 and the Reynolds number is 500; four results are shown: the no-slip flow and three rarefied flows at densities of $10^{-5}\,\mathrm{kg/m^3}$, $10^{-6}\,\mathrm{kg/m^3}$, and $10^{-7}\,\mathrm{kg/m^3}$. Figure 5 is a comparison of the iso-Mach lines obtained with different boundary conditions. Figure 6 is a comparison of the Mach numbers at the edge of the Knudsen layer. It is clear that the boundary condition has a spectacular effect on the results: while the no-slip flow is only weakly transsonic because of the viscous effects, the most rarefied one has all its viscous influence concentrated in the wake and is consequently strongly transsonic, with a maximum Mach number of 1.35.

We then computed a high speed flow over a cylinder, at a Mach number of 8 and a Reynolds number of 1000; four results are presented: the no-slip flow and three rarefied flows at densities of $10^{-4}\,\mathrm{kg/m^3}$, $10^{-5}\,\mathrm{kg/m^3}$, and $10^{-6}\,\mathrm{kg/m^3}$. Figure 7 shows the mesh, which has about 5000 nodes; Fig. 8 shows a comparison of the iso-Mach lines. The viscous boundary layer shrinks up to almost disappearing, except around the detachment point; this reduces the "effective" or "inviscid" thickness of the obstacle and makes the bow shock closer to the wall when the gas is rarefied.

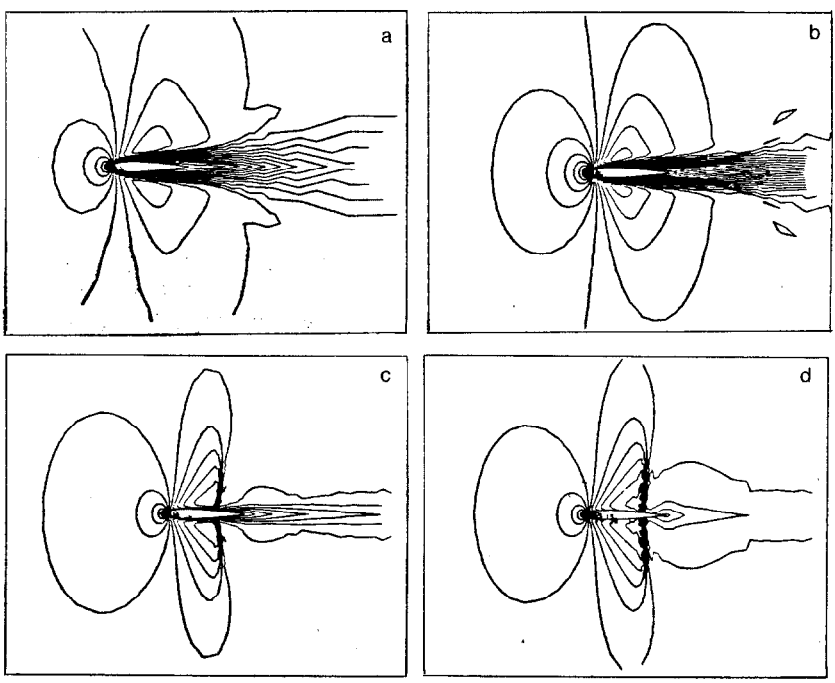

FIG. 5. Iso-Mach lines: (a) No slip; (b) $\rho_\infty = 10^{-5}\,\mathrm{kg/m^3}$; (c) $\rho_\infty = 10^{-6}\,\mathrm{kg/m^3}$; (d) $\rho_\infty = 10^{-7}\,\mathrm{kg/m^3}$.

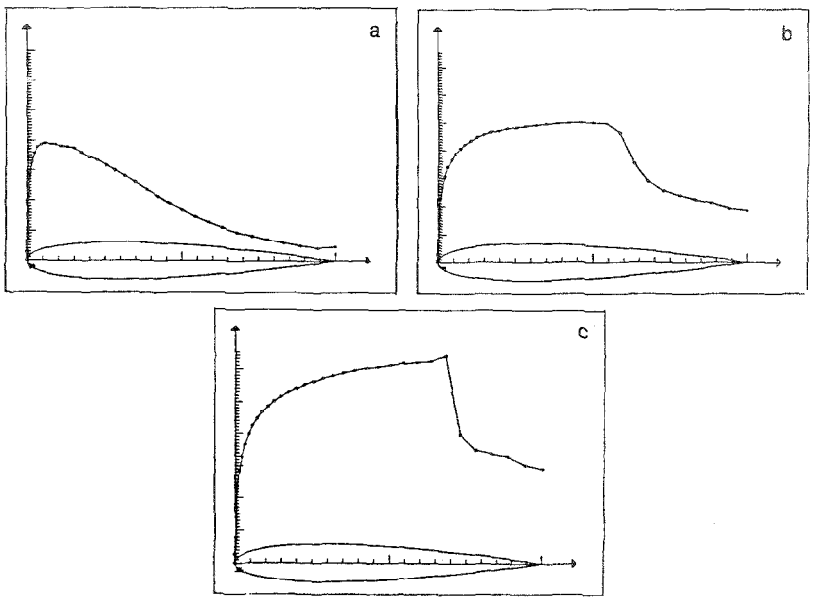

FIG. 6. Mach number on the body: (a) $\rho_\infty = 10^{-5}\,\mathrm{kg/m^3}$; (b) $\rho_\infty = 10^{-6}\,\mathrm{kg/m^3}$; (c) $\rho_\infty = 10^{-7}\,\mathrm{kg/m^3}$.

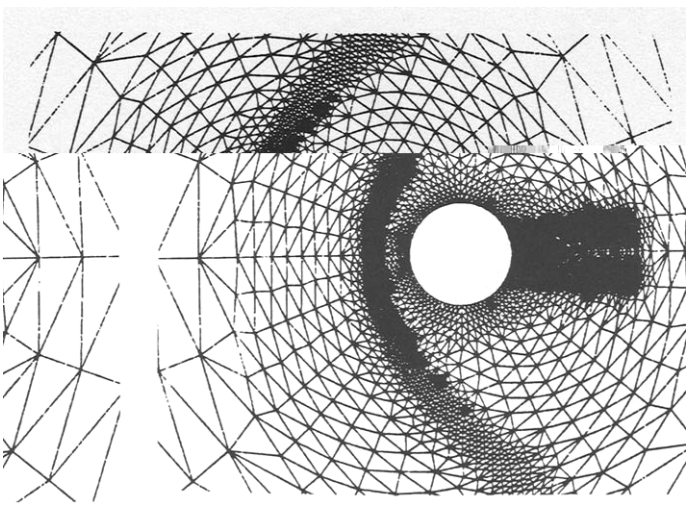

FIGURE 7

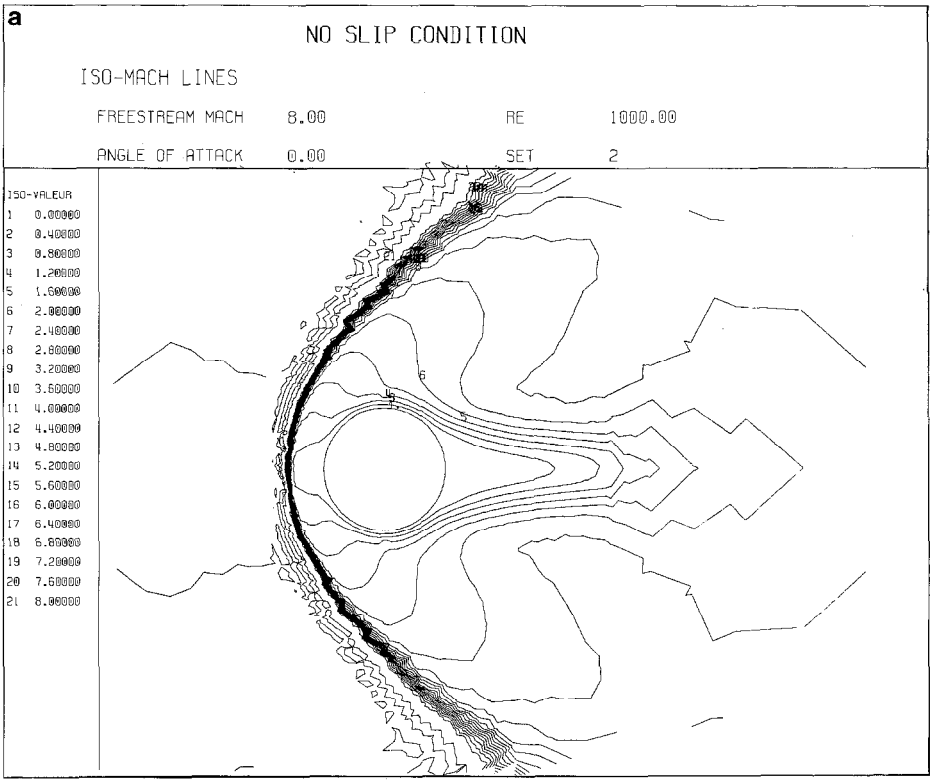

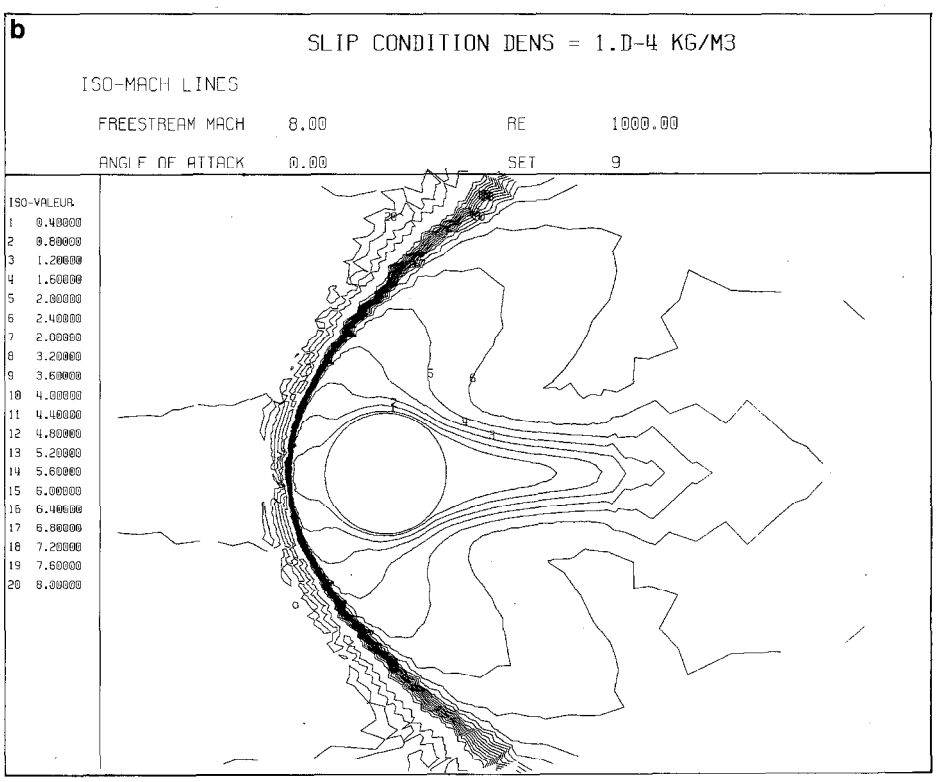

FIG. 8. Iso-Mach lines: (a) No slip; (b) $\rho_\infty = 10^{-4}$ kg/m^3; (c) $\rho_\infty = 10^{-5}$ kg/m^3; (d) $\rho_\infty = 10^{-6}$ kg/m^3.

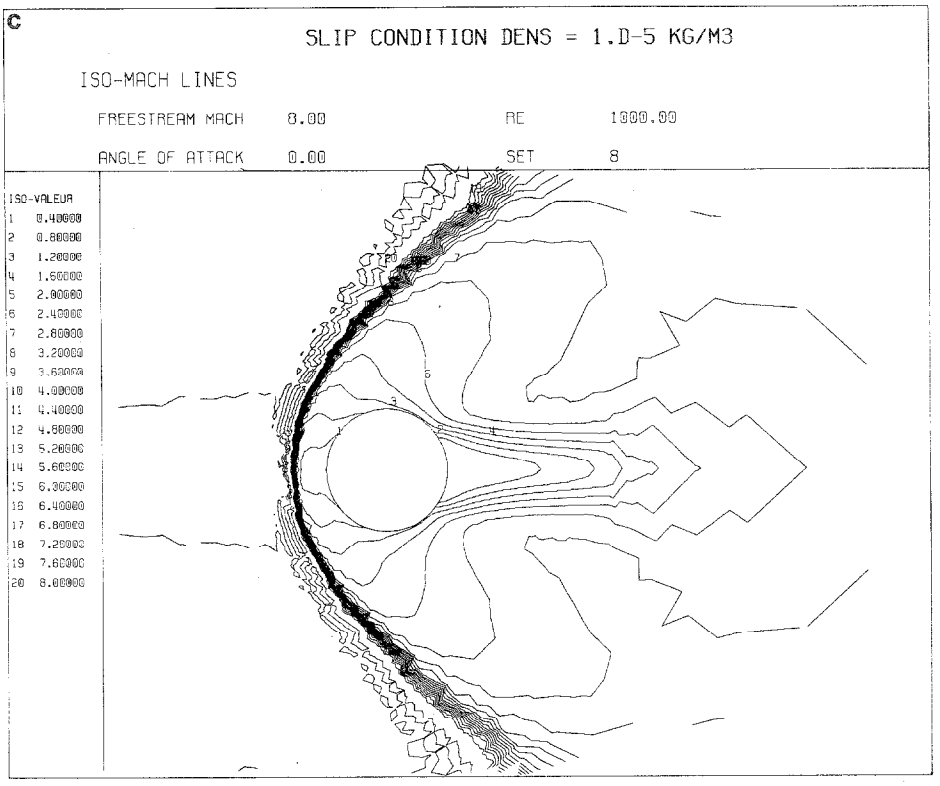

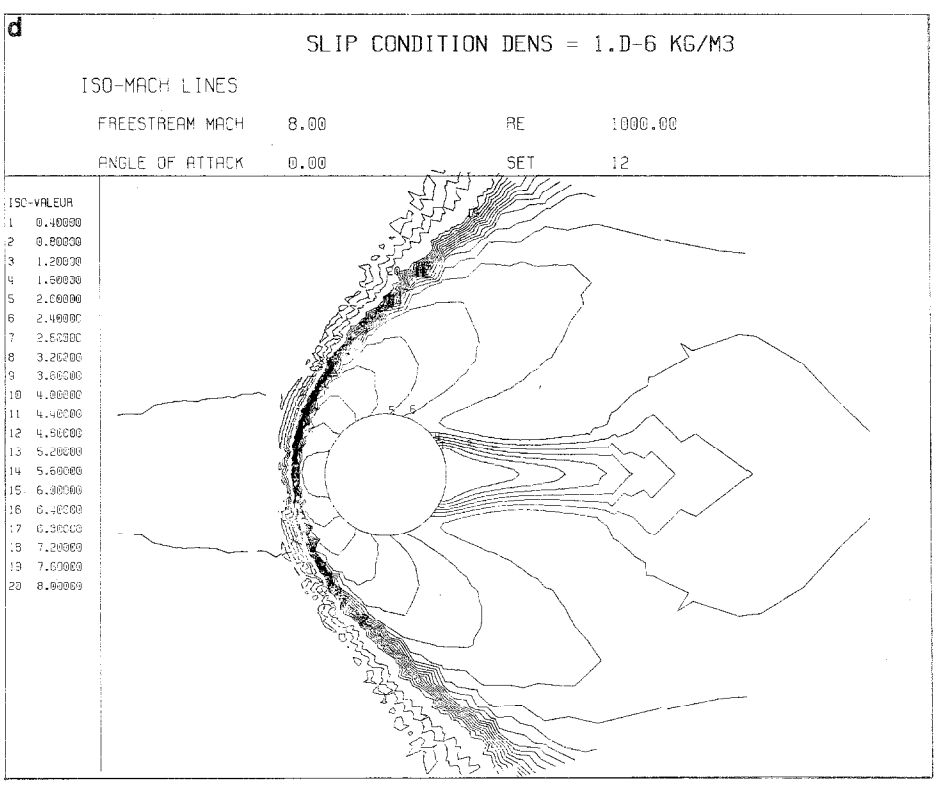

FIG. 8—*Continued*

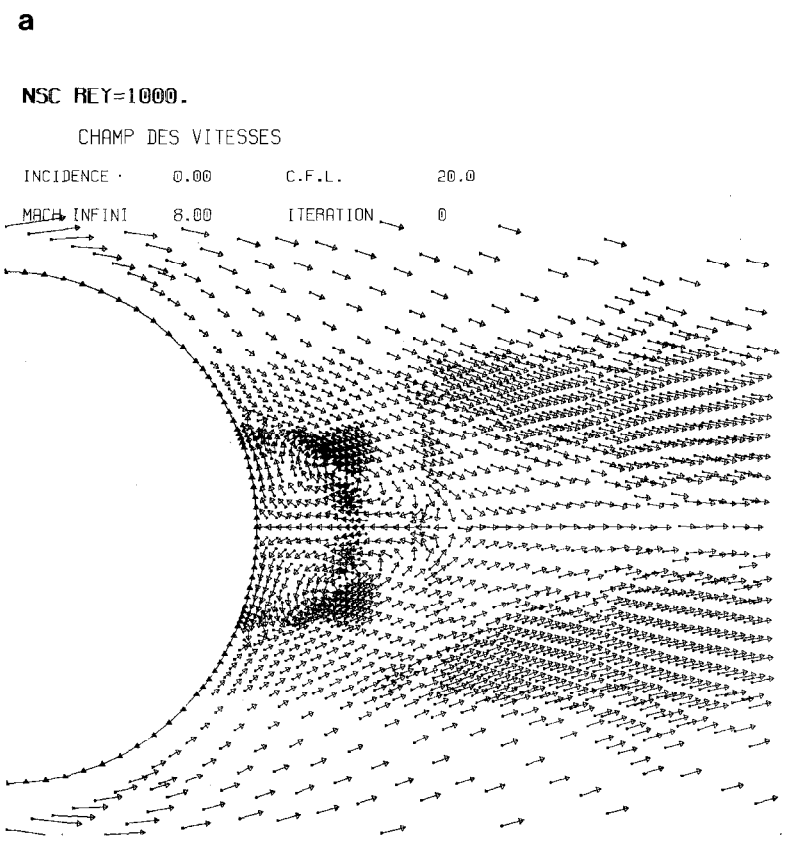

FIG. 9. Speed vectors directions behind the cylinder: (a) No slip, (b) $\rho_\infty = 10^{-4}\,\mathrm{kg}/m^3$; (c) $\rho_\infty = 10^{-5}\,\mathrm{kg}/m^3$; (d) $\rho_\infty = 10^{-6}\,\mathrm{kg/m^3}$.

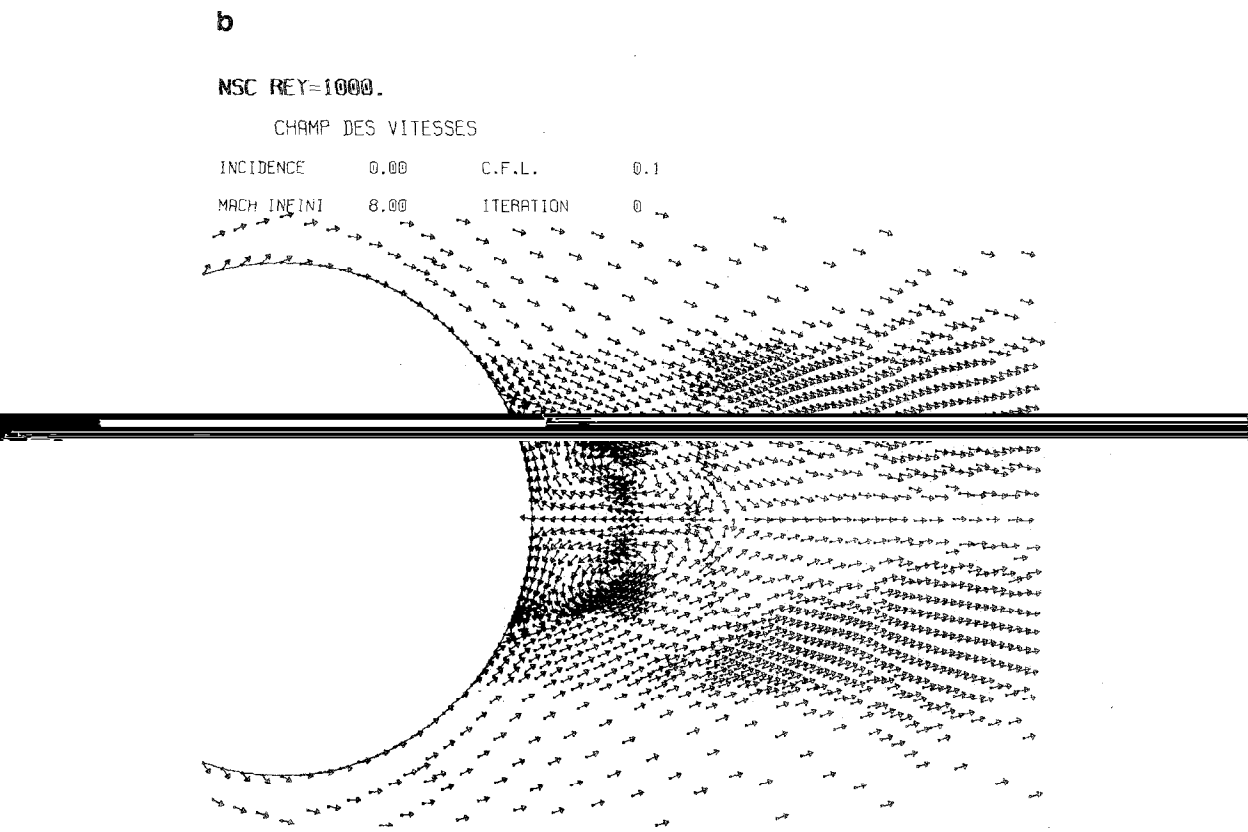

FIG. 9—*Continued*

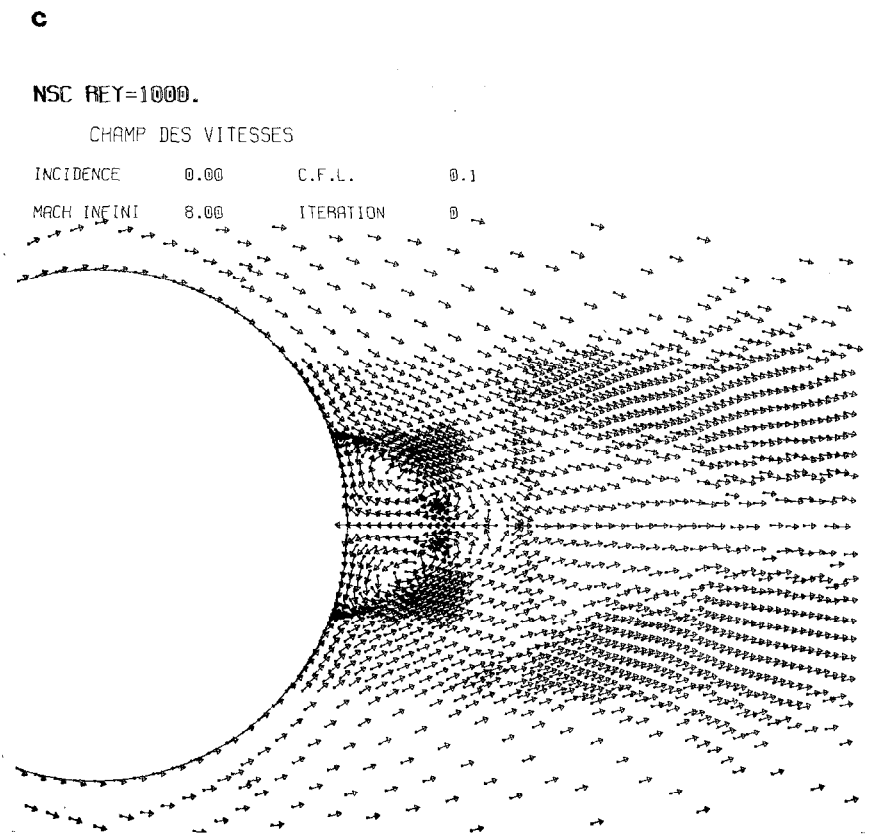

FIG. 9—*Continued*

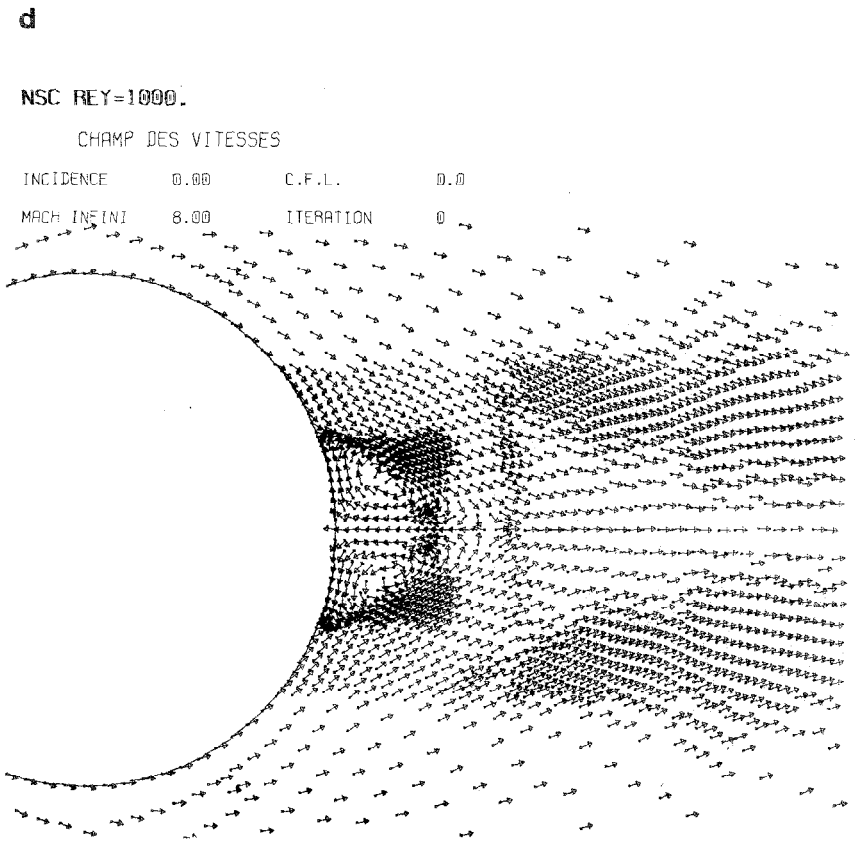

FIG. 9—*Continued*

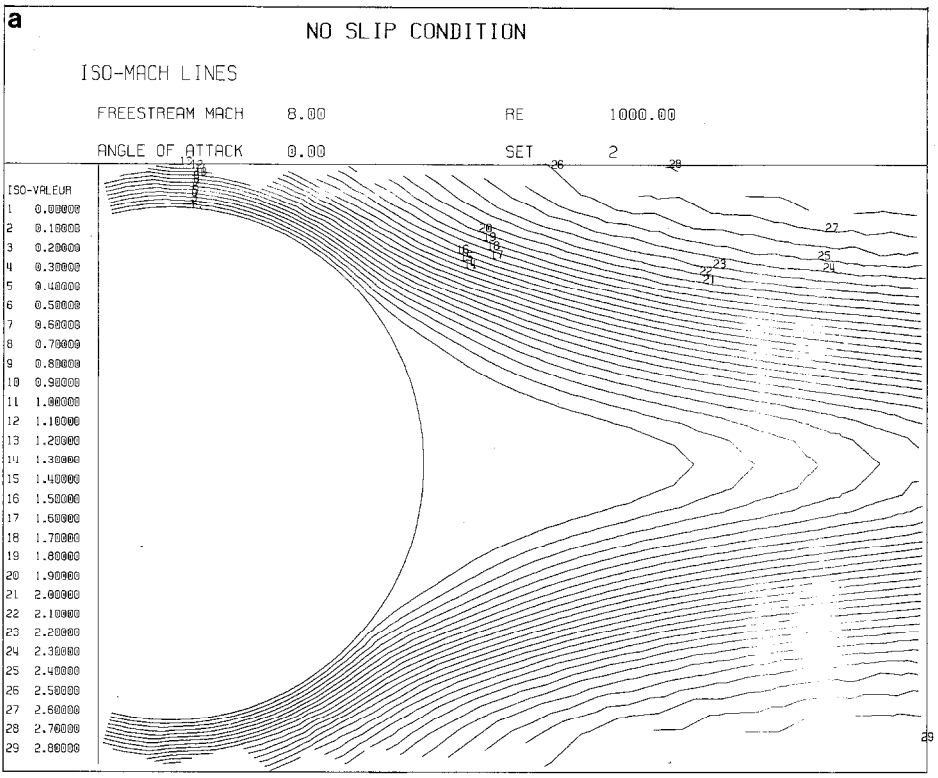

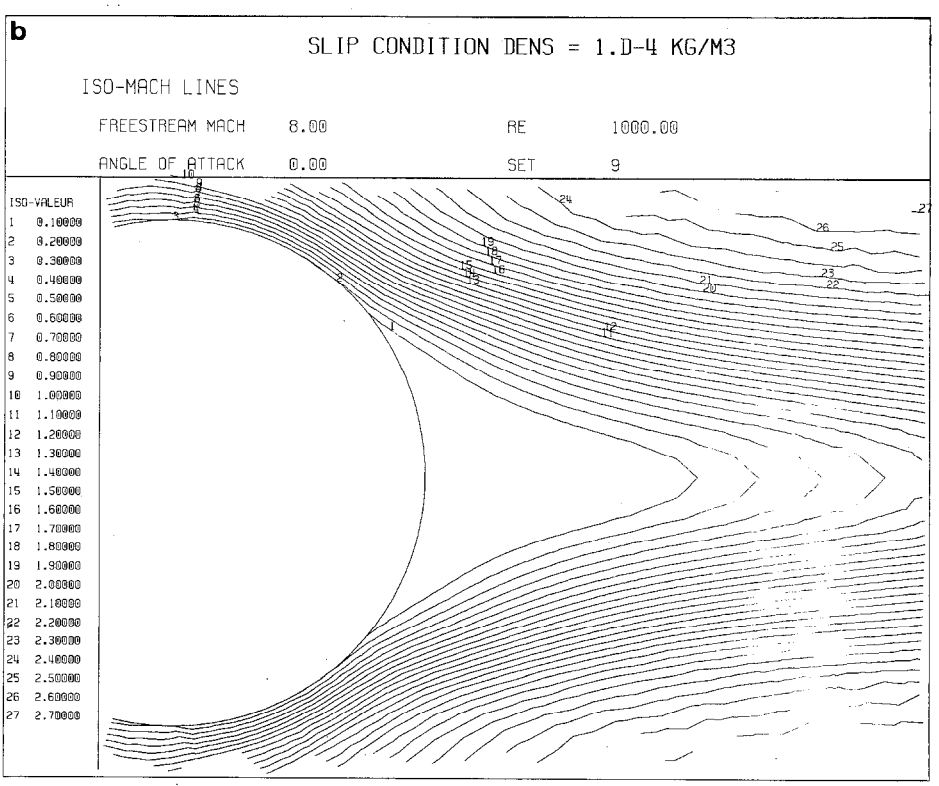

FIG. 10. Enlargement of the iso-Mach lines: (a) No slip; (b) $\rho_\infty = 10^{-4}$ kg/m^3; (c) $\rho_\infty = 10^{-5}$ kg/m^3; (d) $\rho_\infty = 10^{-6}$ kg/m^3.

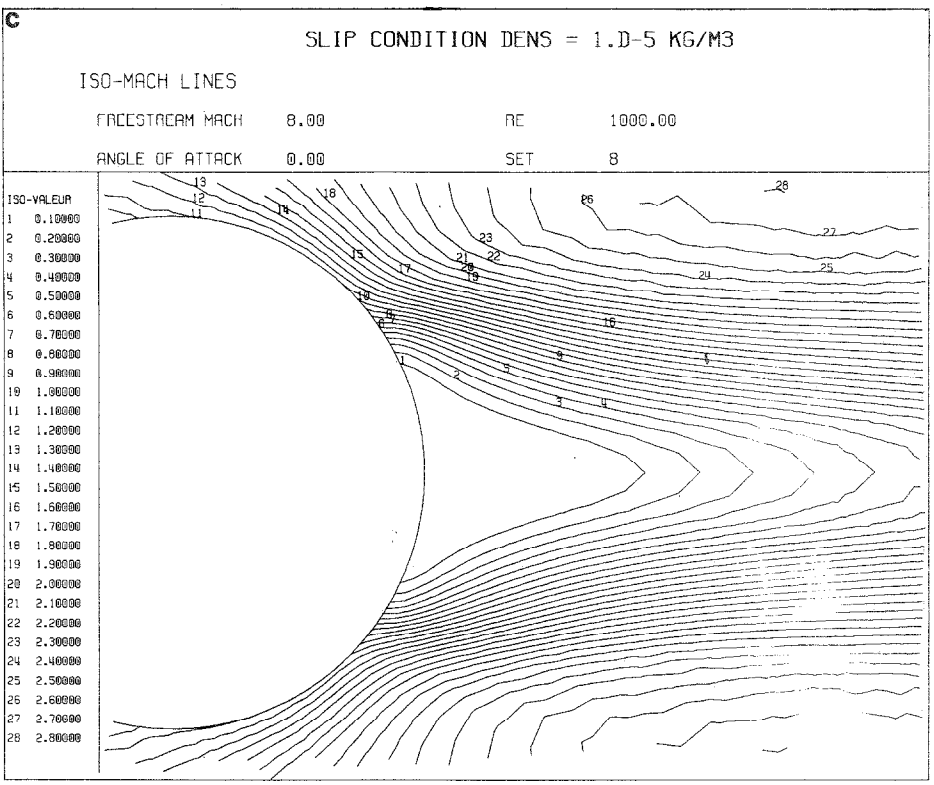

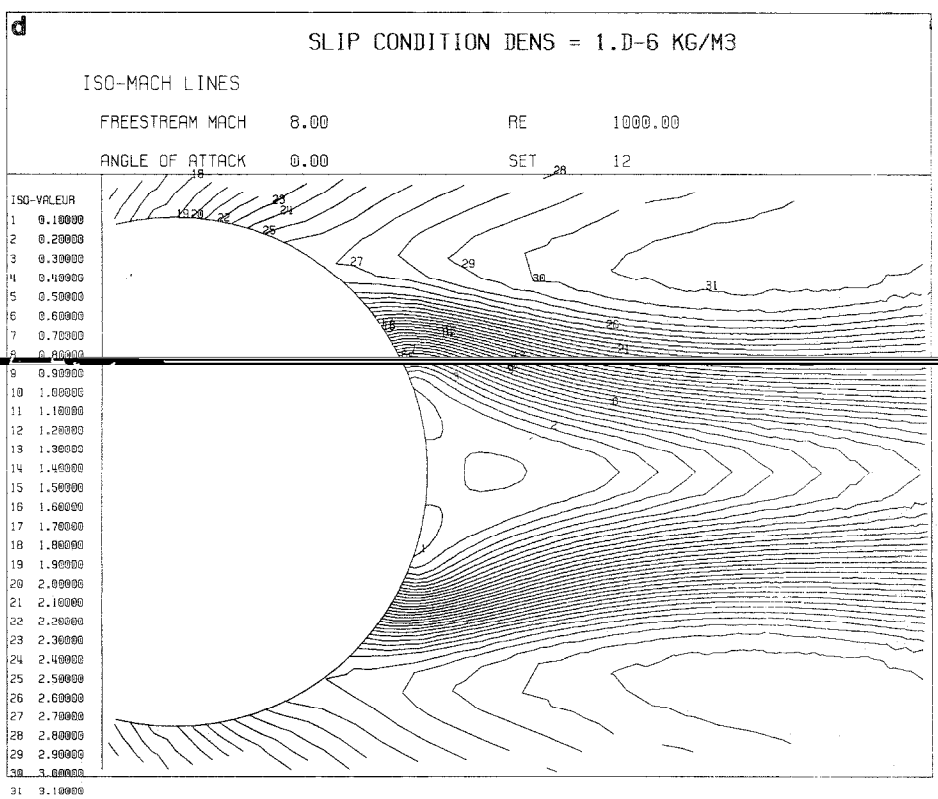

FIG. 10—*Continued*

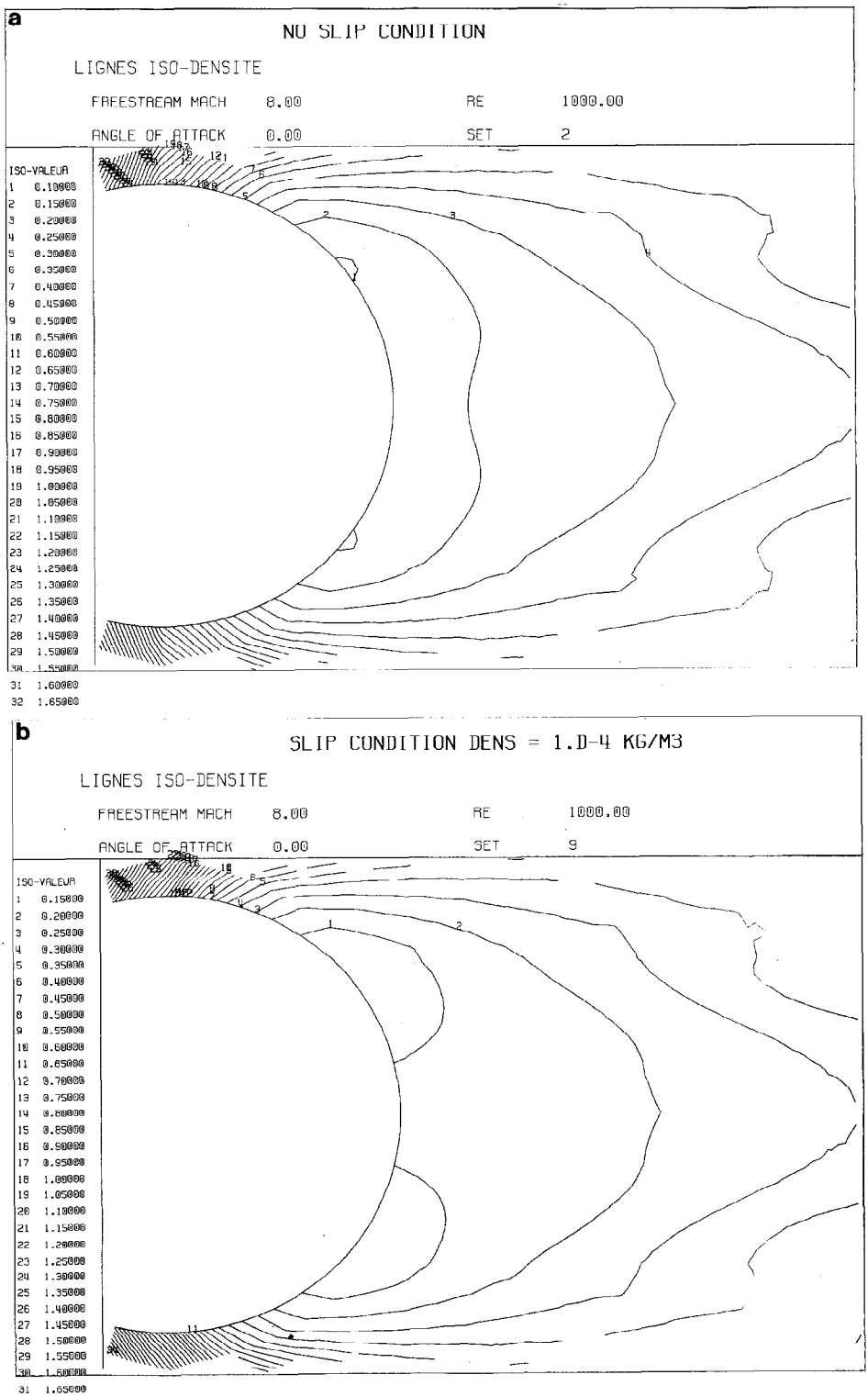

FIG. 11. Enlargement of iso-density lines: (a) No slip; (b) $\rho_\infty = 10^{-4}$ kg/m^3; (c) $= 10^{-5}$ kg/m^3; (d) $\rho_\infty = 10^{-6}$ kg/m^3.

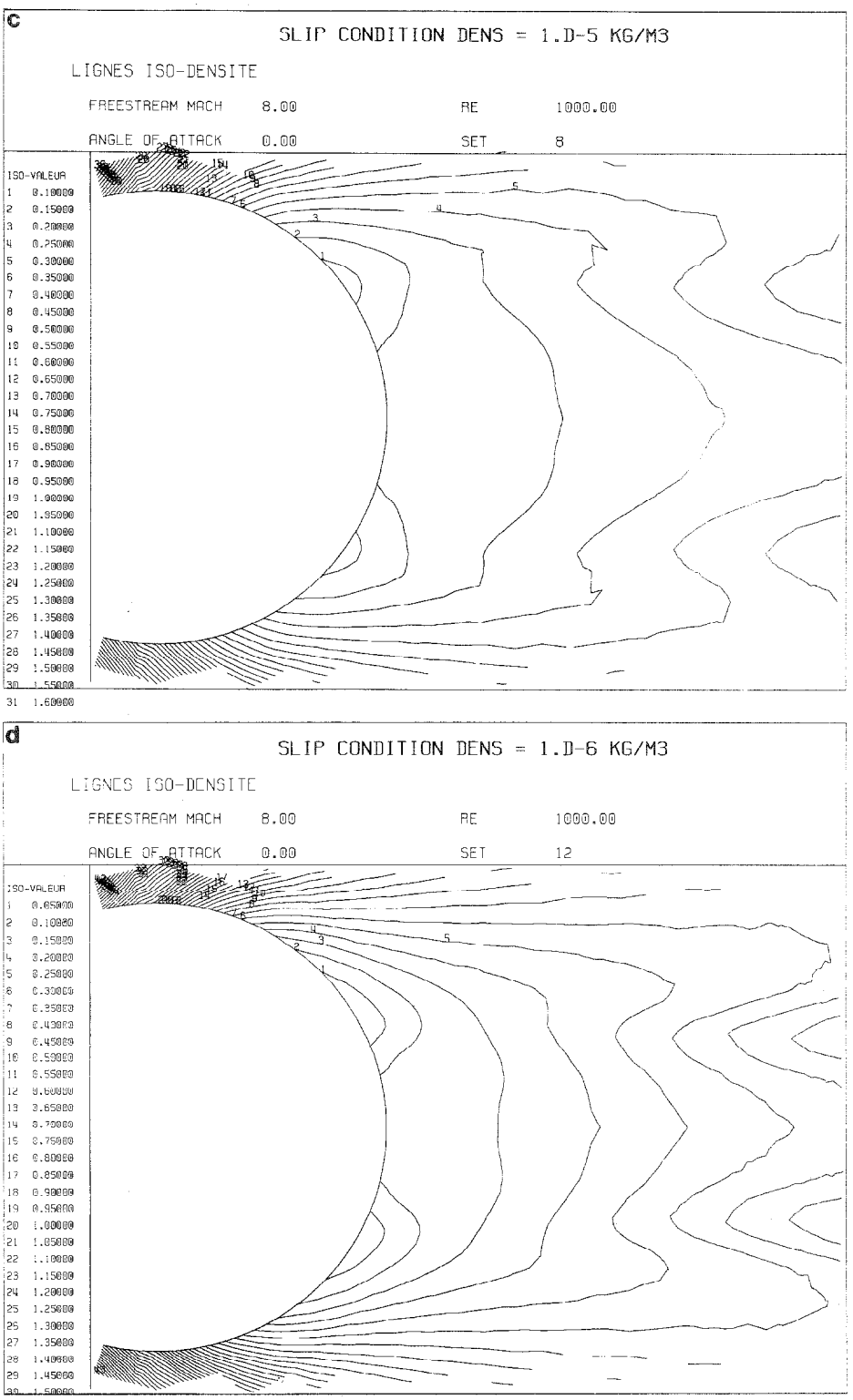

FIG. 11—*Continued*

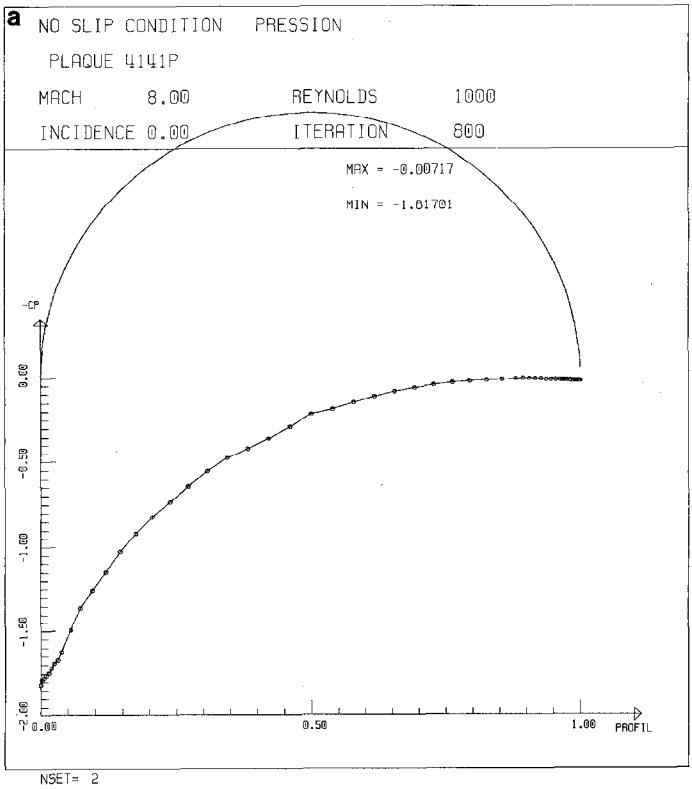

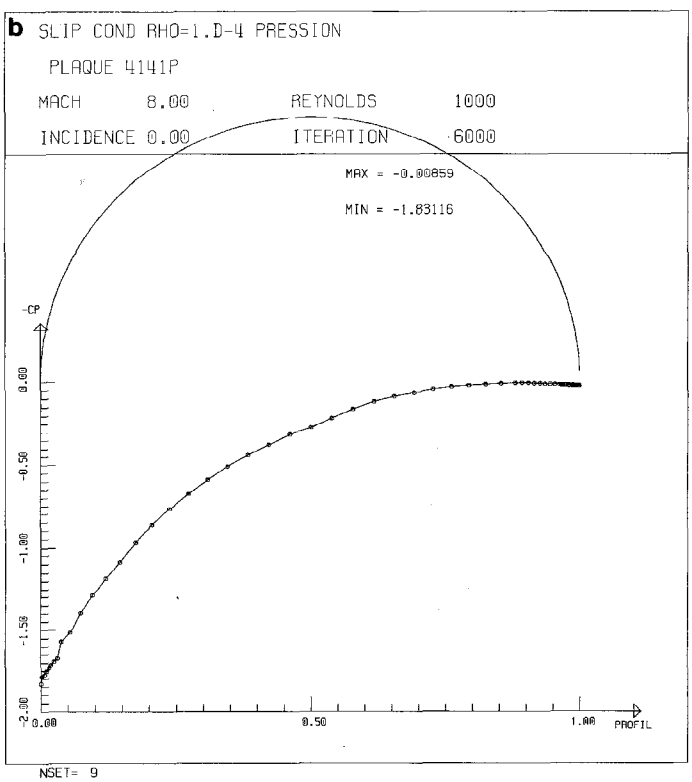

FIG. 12. Pressure coefficient on the body: (a) No slip; (b) $\rho_\infty = 10^{-4}$ kg/m^3; (c) $\rho_\infty = 10^{-5}$ kg/m^3; (d) $\rho_\infty = 10^{-6}$ kg/m^3.

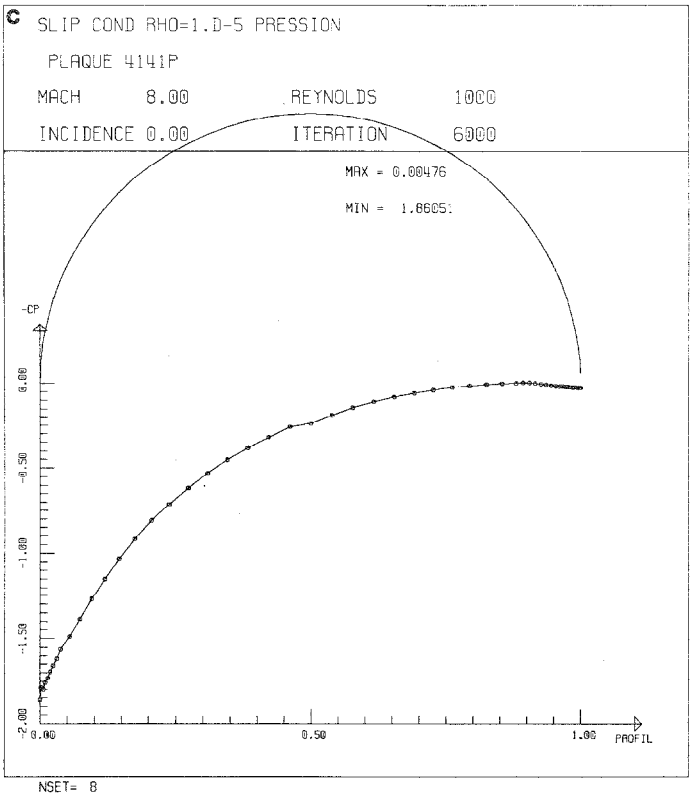

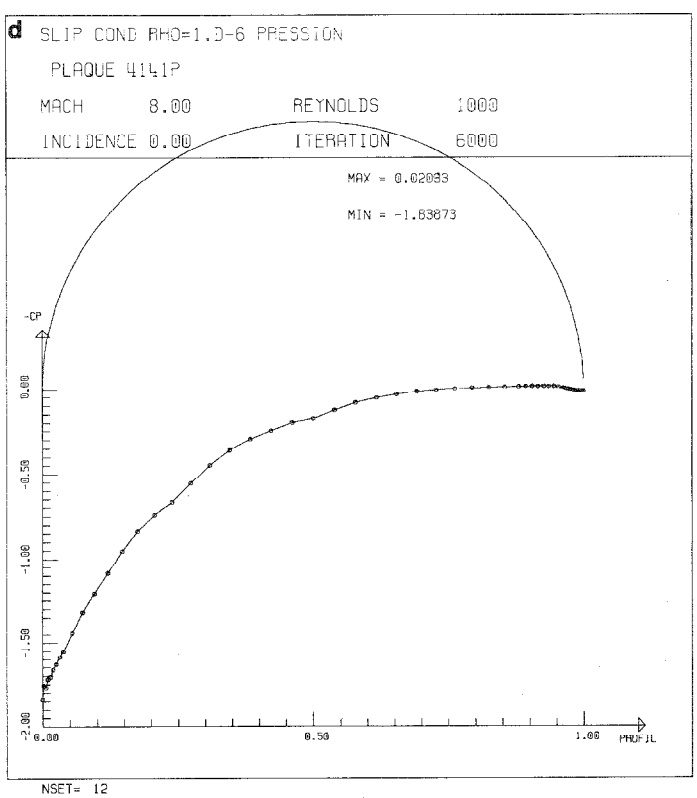

FIG. 12—*Continued*

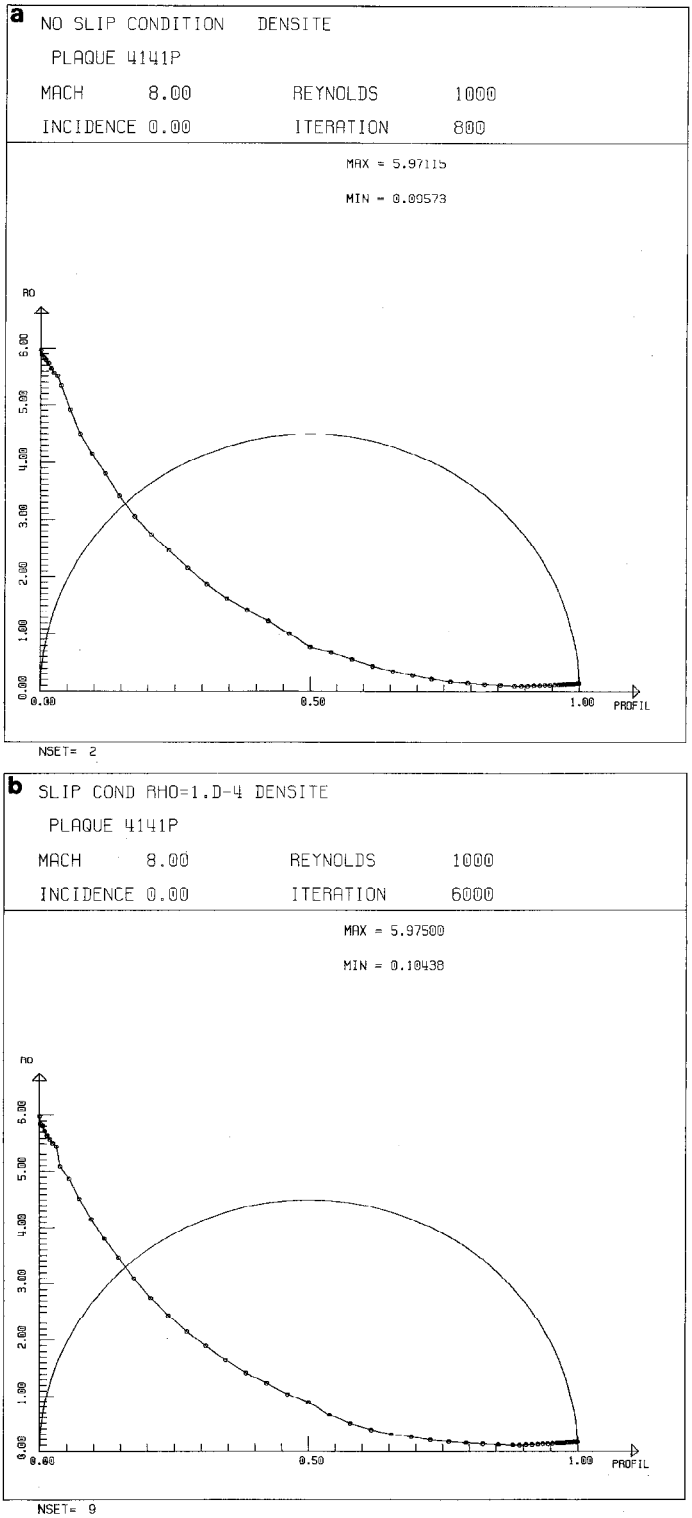

FIG. 13. Density on the body (ρ/ρ_∞): (a) No slip; (b) $\rho_\infty = 10^{-4}\,\mathrm{kg/m^3}$; (c) $\rho_\infty = 10^{-5}\,\mathrm{kg/m^3}$; (d) $\rho_\infty = 10^{-6}\,\mathrm{kg/m^3}$.

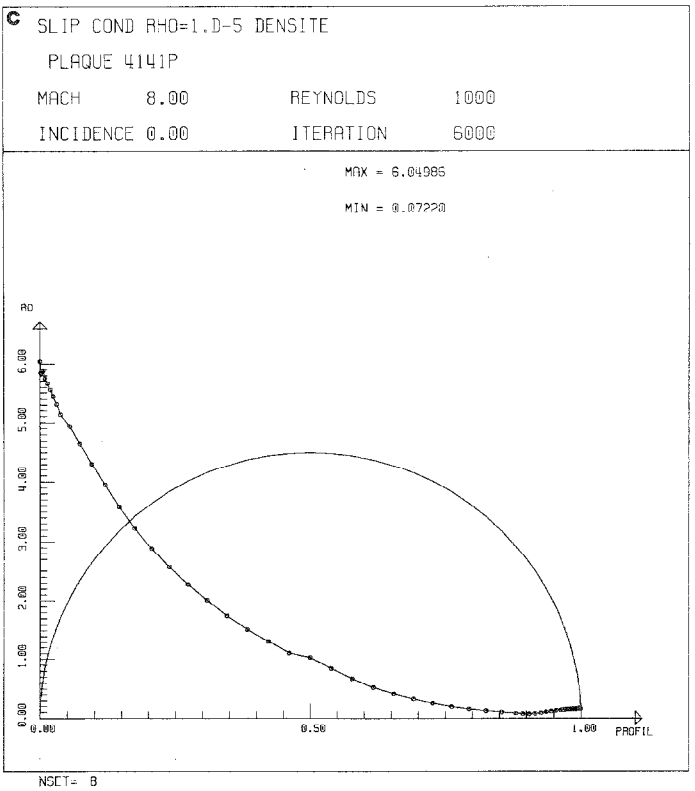

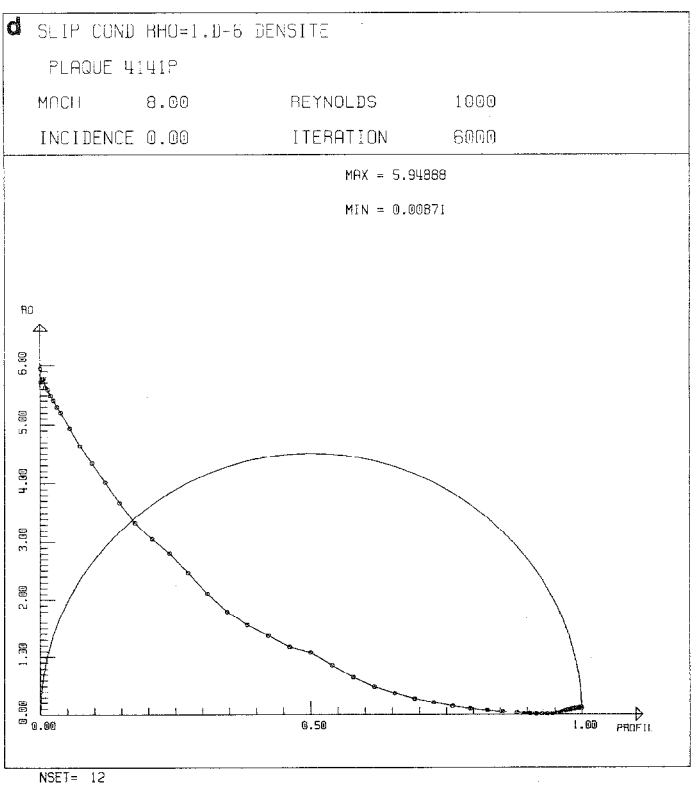

FIG. 13—*Continued*

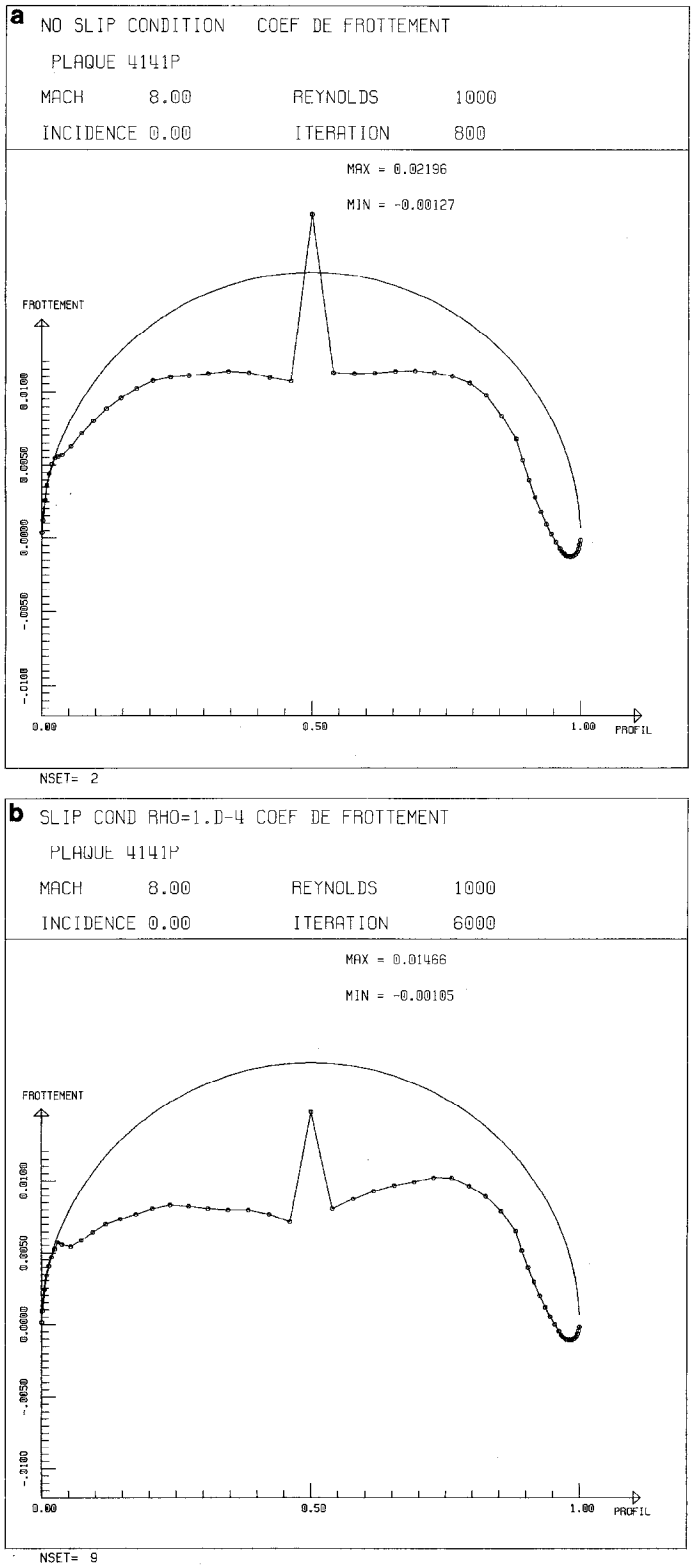

FIG. 14. Skin friction coefficient: (a) No slip; (b) $\rho_\infty = 10^{-4}\,\mathrm{kg/m^3}$; (c) $\rho_\infty = 10^{-5}\,\mathrm{kg/m^3}$; (d) $\rho_\infty = 10^{-6}\,\mathrm{kg/m^3}$.

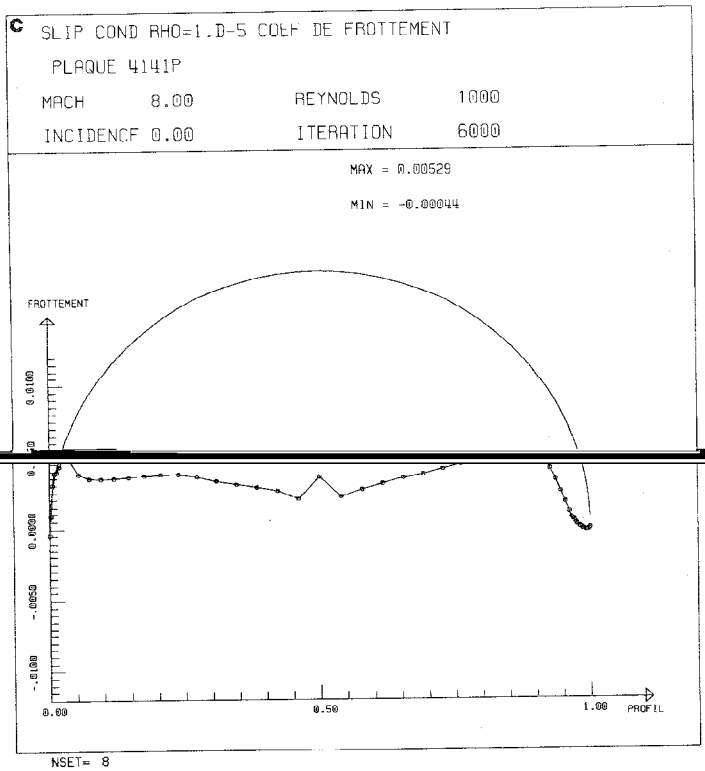

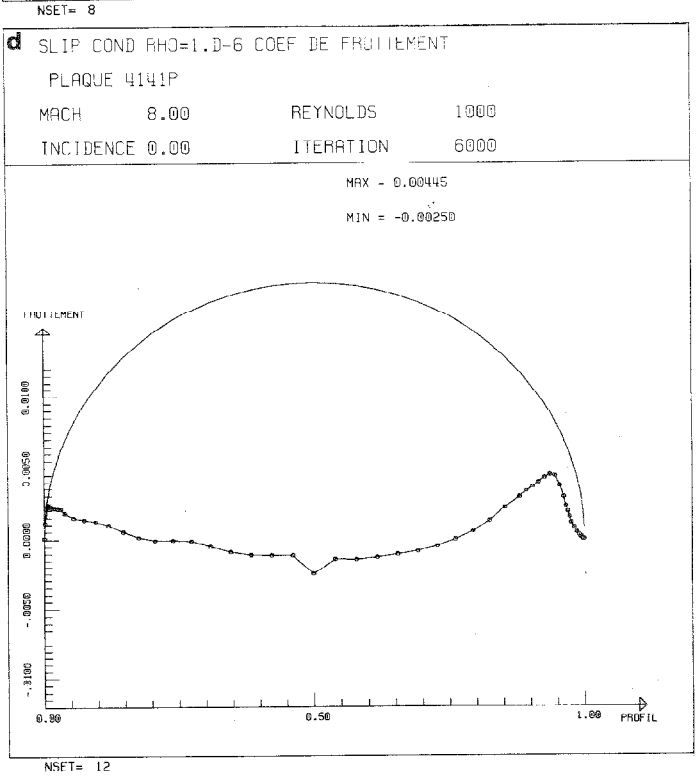

FIG. 14—*Continued*

The recirculation zone between the wall and the stagnation point is smaller for rarefied flows, moving with decreasing densities to the perfect gas solution. Figures 9, 10, and 11 are comparisons of the rear body flows. Figures 12, 13, and 14 are plot of the pressure, density, and friction at the edge of the Knudsen layer. Pressure and density are not much affected by the boundary conditions, but the friction decreases quickly as density decreases, which is the awaited behaviour.

CONCLUSION

Significative differences appear between slip and no-slip simulations, the former seeming to be closer to experimental results. Bow shocks are closer to the obstacles for slip flows, as indicated by experiment, and the slip boundary conditions give more generally solutions in better qualitative agreement with the awaited behaviours. Nevertheless, more accurate comparison with experiment will have to be made before the model can be tuned and validated.

The slip boundary conditions have been shown to be well posed in the sense of conservation. They have been included in a numerical scheme to solve the compressible Navier–Stokes equations, at no major increase in computational cost.

ACKNOWLEDGMENTS

This work owes much to F. Angrand, M. O. Bristeau, O. Pironneau of INRIA, and to B. Mantel, J. Periaux, and B. Stoufflet of AMD-BA whom I want to thank here. The author is supported by DRET Contract n 03 40 79 01.

REFERENCES

1. J. ALLÈGRE, M. RAFFIN, AND L. GOTTESDIENER, Slip effects around NACA0012 airfoils, SESSIA, Meudon, France, private communication (1985).
2. R. GUPTA, C. SCOTT, AND J. MOSS, NASA Technical Paper 2452, 1985 (unpublished).
3. F. CORON, F. GOLSE, C. SULEM, A classification of well-posed kinetic layer problems, parts I and II, private communication (1987).
4. R. BRUN, *Transport et relaxation dans les écoulements gazeux* (Masson, Paris, 1986).
5. S. CHAPMAN AND T. COWLING, *The Mathematical Theory of Nonuniform Gases* (Cambridge Univ. Press, London, 1952).
6. J. O. HIRSCHFELDER, C. F. CURTISS, AND R. B. BIRD, *Molecular Theory of Gases and Liquids* (Wiley, New York, 1967).
7. G. A. BIRD, *Molecular Gas Dynamics* (Oxford Univ. Press, London, 1976).
8. C. BARDOS, Equations cinétiques et approximations fluides, Cours de DEA, Université Paris VI, 1986–87 (unpublished).
9. S. MAS-GALLIC, *Transport theory and statistical physics*, to appear.
10. C. CERCIGNANI, *Theory and Applications of the Boltzman Equation* (Scottish Academic Press, Edinburgh, 1975).
11. A. VALLI, *Ann. Math. Pura Appl.* (IV) **130**, 197 (1).

12. R. VERFURTH, Thesis, Ruhr Universitat, Bochum, June 1986 (unpublished).
13. J. A. NITSCHE, *RAIRO Anal. Num.* **15**, 237 (1981).
14. M. O. BRISTEAU AND J. PÉRIAUX, in *Lecture Notes on Computational Fluid Dynamics, March* 3–7, 1986, Von Karman Institute for Fluid Dynamics.
15. F. ANGRAND, in *Proceedings of the GAMM Workshop on Viscous Compressible Fluids, Nice,* 1984 (unpublished).
16. F. ANGRAND AND A. DERVIEUX, *Int. J. Num. Methods Fluids* **4**, 749 (1984).
17. B. STOUFFLET, Thesis, Université Paris VI, 1984 (unpublished).
18. B. STOUFFLET, J. PERIAUX, L. FEZZOUI, AND A. DERVIEUX, *AIAA Paper* 87 0560, Reno, 1987.